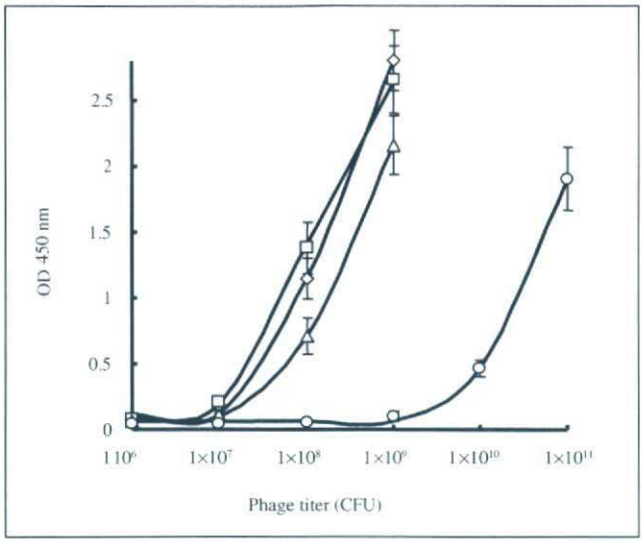

Fig. 3: Comparison of the efficiency of protein-display using pIII type phage display.
The efficiency of protein-display on pIII was assessed by phage ELISA. Proteins with different molecular weights (approximately 400–58,000 Da) were displayed on phage particle as pIII fusion proteins. This experiment was performed using the same method as Fig. 2 (n = 3). Each data value represents the mean ± S.D. □, RGDS-pIII phage; ◇, LacZ-pIII phage; △, scFv-pIII phage; ○, Importin-α-pIII phage

ated the relationship between electric charge and display efficiency using FLAG tagged ELISA (Fig. 2A). The display of positively charged SV40 NLS and HIV-1 Tat peptides were less efficient than that of the neutrally charged RGDS peptide. Generally, positively charged peptides are easy to adsorb onto various surfaces (Gaillard et al. 1999), and they repulse each other. Therefore, positively charged peptides may interfere with phage assembly in the periplasm.

Second, we examined the relationship between molecular weight and display efficiency again using FLAG tagged ELISA (Fig. 3). Because the display of positively charged sample was less efficient (Fig. 2), we used the neutrally charged proteins (pI 5.0–6.4) (MW 1.5–58 kDa) displayed on pIII to examine the influence of molecular weight on display. Phage displaying the low molecular weight RGDS peptide bound to anti-FLAG antibody at a concentration of 10^6–10^9 CFU. The higher molecular weight importin-α (58 kDa) displayed on the phage surface could not bind at the same concentration, needing 10^9–10^{11} CFU. In general, the amount of phage prepared by following the standard protocol was approximately 10^{12}–10^{13} CFU (Imai 2006). To create functional mutants using a phage library, it is desirable to use an amount of phage in excess (more than 100-fold) of the phage library (approximately 10^6–10^9 CFU). When proteins display on the phage surface efficiently, the experiment can proceed without bias. However, our result suggests that a phage library displaying high molecular weight proteins may be of low quality simply because the levels of the desired proteins are not sufficiently expressed for screening. This introduces a selection bias for those proteins that can be expressed at the proper level.

To examine the efficiency of pIII-display in greater detail, we quantified the number of molecules displayed on the phage surface by electrophoresis analysis using CsCl purified phage (Fig. 4). These results (Fig. 3, 4) demonstrate that the efficiency of RGDS peptide-display on pIII was the best (approximately 2 molecules/phage). The display efficiency decreased as the molecular weight of the target protein increased. Because the titer of all phages prepared in this experiment was determined, we suggested that the display of different molecular weight proteins did not affect the efficiency of phage-preparation (data not shown). Additionally, the proteins used in this experiment (RGDS, LacZ, scFv and importin-α) were expressed efficiently in *E. coli*. Therefore, we suggest that the efficiency with which a protein is displayed on pIII is directly related to its molecular weight.

Finally, we examined the efficiency of pVIII-display by Western blot and confirmed that it also decreased as the molecular weight increased (Fig. 5). Interestingly, this result shows that scFv (25 kDa) could be displayed on pVIII efficiently. Because the pVIII phage display system is generally believed to be limited in its application precisely by the molecular weight of displayed protein, many used it only for display of peptide libraries (Verhaert et al. 1999; Kneissel et al. 1999; Lowman 1997; Gaillard et al. 1999). However, our result suggests that the pVIII system could be applied to larger molecules. This could provide useful

A)

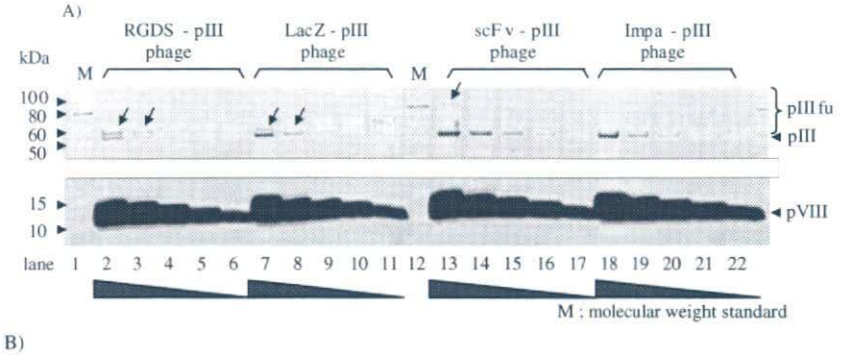

B)

	RGDS-pIII	LacZ-pIII	scFv-pIII	Impα-pIII
M.W. of displayed protein (kDa)	1.5	11	25	58
M.W. of pIII fusion protein (kDa)	52.5	62	76	109
Number of displayed proteins/phage	2.7	1.0	0.12	N.D.

N.D.; Not Detectable

Fig. 4:
Calculated quantity of pIII displayed proteins using Sypro® Ruby staining.
A) The efficiency of display on pIII was quantified using CsCl purifed phages. RGDS-pIII (lanes 2–6), LacZ-pIII (lanes 7–11), scFv-pIII (lanes 13–17) and Impα-pIII phage (lanes 18–22) were used in this experiment. Molecular weight standard was loaded in lanes 1 and 12. Starting from the left, 1×10^{13} vp, 3.3×10^{12} vp, 1.1×10^{12} vp, 3.7×10^{11} vp and 1.2×10^{11} vp were loaded. B) The number of displayed proteins per one phage particle was calculated by fluorescence image analysis. Fluorescence intensity was quantified by Typhoon image analyzer

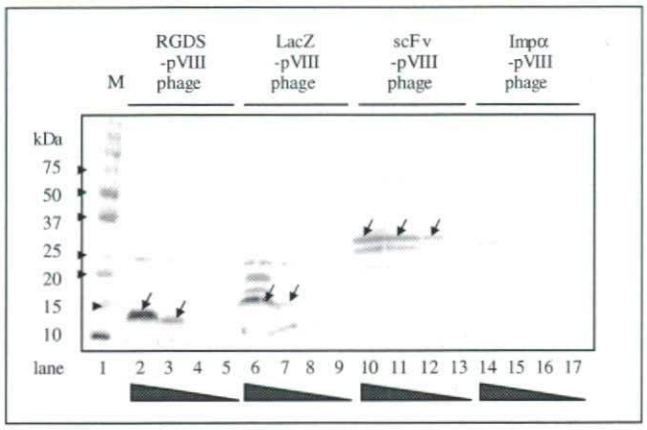

Fig. 5: Comparison of the efficiency of pVIII display protein on phage particles.
The efficiency of display on pVIII was assessed by anti-FLAG western blot. PEG-purified RGDS-pVIII (lanes 2–5), LacZ-pVIII (lanes 6–9), scFv-pVIII (lanes 10–13) and Impα-pVIII phage (lanes 14–17) were used in this experiment. Molecular weight standard was loaded in lane 1. Starting from the left, 1.5×10^{11} cfu, 5×10^{10} cfu, 1.7×10^{10} cfu and 5.5×10^{9} cfu were loaded

additional information by expanding the application of phage display systems to create various mutant proteins.
In this study, different kinds of sample peptides (SV40 NLS, HIV-1 Tat, RGDS) and proteins (RGDS, LacZ, scFv, importin-α) that could be readily expressed in *E. coli* were used as model molecules. The display of positively charged SV40 NLS and HIV-1 Tat peptides on pIII was less efficient than that of the neutrally charged RGDS peptide. When different molecular weight proteins (1.5–58 kDa) were displayed on pIII and pVIII, their display efficiencies were directly related to their molecular weights.
When comparing the efficiency of display between the four model proteins, additional factors (i.e. refolding efficiency, etc.) may account for the differences. These results show at least that the electric charge affected the efficiency of phage display and that high molecular weight proteins could not be displayed on the phage surface successfully. Recently, it was reported that improving the phagemid vector provided better efficiency of protein refolding in *E. coli* and enhanced protein display on the phage surface (Guo et al. 2003). Consequently many hope that the display efficiency of various molecules could be improved using this methodology. However, while this method improves the quality of fusion protein expression, it does not take into account the efficiency of protein assembly for the construction of phage particles. Therefore, it is still important to be able to predict the molecules that will be compatible for protein and peptide engineering using phage display by understanding the properties of this system as they were described in this report.

3. Experimental

3.1. Phagemid vectors and inserts

The pY03′-FLAG phagemid vector was modified from pCANTAB-5E (GE Healthcare Ltd.). To create this vector, the E-tag from the original vector was changed to a FLAG tag (DYKDDDDK). The pY10-FLAG phagemid vector was constructed by replacing the pIII gene in pY03′-FLAG with the pVIII gene. Genes encoding peptides (RGDS, HIV-Tat, SV40 NLS) were synthesized by Operon Biotechnologies Inc., USA. The lacZ-α gene had already been cloned into pY03′-FLAG and pY10-FLAG. The anti-KDR scFv gene was isolated from an optimized non-immune phage antibody library previously described (Imai et al. 2006). The human importin-α gene was amplified from a human bone marrow cDNA library (TAKARA Bio. Inc.). These inserts were digested and cloned into each phagemid vector.

3.2. Phage preparation

Phage was prepared by following a standard protocol. Briefly, phage particles were prepared from *Escherichia coli* (TG1 strain, Stratagene corporation) by co-infection with M13KO7 helper phage (Invitrogen Corporation). Amplified phage in culture media was roughly purified by PEG precipitation. Part of the purified phage was added to the TG1 bacteria, and the phage titer (cfu) was calculated by counting infected TG1 colonies. If necessary, additional purification using a CsCl gradient was performed as described below.

3.3. Phage ELISA

Immunoplates (Nalge Nunc International) were immobilized with anti-FLAG M2 antibody (Sigma-Aldrich Corporation) diluted to 5 μg/ml in bicarbonate buffer (Sigma-Aldrich Corporation). Plates were blocked with 2% block ace (Nakarai Tesque Inc.) for 2 h at 37 °C. Phage solution (PEG-purified) in 0.4% block ace was serially diluted and applied to the wells. After a 1 h incubation at room temperature, the binding phage was detected by anti-M13 HRP conjugate (GE Healthcare Ltd.).

3.4. Purification of phage particles under CsCl gradient

Amplified phage was purified by PEG precipitation. Phage pellets were resuspended in TBS buffer. CsCl powder (IWAI chemicals company) and additional TBS buffer were added to the phage solution up to 31%. After CsCl gradient ultracentrifugation at 400,000 × g at 5 °C for 20 h, the concentrated phage band was isolated. TBS (five volumes) was added to the purified phage and centrifuged again at 400,000 × g at 5 °C for 4 h to remove the CsCl. The obtained phage was resuspended in TBS and used for experiments.

3.5. Sypro Ruby staining

After purifying the phage under a CsCl gradient, the number of phage particles (vp/ml) was estimated from its absorbance according to the standard protocol. Serially diluted phage samples were resolved by SDS – poly acrylamide electrophoresis (SDS-PAGE). Gels were incubated in SYPRO® Ruby protein gel stain reagent (Pearce Biotechnology, Inc., USA) overnight at room temperature. After washing with wash buffer (10% methanol and 7% acetic acid) for 30 min, fluorescence was detected using the Typhoon Variable Image Analyzer (GE Healthcare Ltd.). The number of surface-displayed proteins was calculated from fluorescence intensity using ImageQuant TL software (GE Healthcare Ltd.) assuming that one phage particle contained five pIII coat proteins on its surface.

3.6. Anti-FLAG western blotting

SDS-PAGE was performed using serially diluted phage purified by PEG precipitation. Phage protein in the gel was transferred to PVDF membrane (GE Healthcare Ltd.) using the Hoefer TE 70 semi dry transfer unit (GE Healthcare Ltd.). Membranes were blocked in 4% block ace for 1 h. FLAG-tagged pVIII fusion protein was detected with anti-FLAG M2 antibody (Sigma-Aldrich Corporation) and anti-mouse IgG HRP conjugate (Sigma-Aldrich Corporation). After detection by ECL plus reagent (GE Healthcare Ltd.), its luminescence was quantitated using the LAS-3000 Lumi Imager (Fujifilm Corporation).

Acknowledgements: This study was supported in part by Grants-in-Aid for Scientific Research (No. 20015052) from the Ministry of Education, Culture, Sports, Science and Technology of Japan, by Health and Labor Sciences Research Grant from the Ministry of Health, Labor and Welfare of Japan, and in part by Research Fellowships for Young Scientists (No. 3608) from Japan Society for the Promotion of Science.

References

Bayer R, Feigenson GW (1985) Reconstitution of M13 bacteriophage coat protein. A new strategy to analyze configuration of the protein in the membrane. Biochim Biophys Acta 815: 369–379.
Chasteen L, Ayriss J, Pavlik P, Bradbury AR (2006) Eliminating helper phage from phage display. Nucleic Acids Res 34: e145.
Gaillard C, Flavin M, Woisard A, Strauss F (1999) Association of double-stranded DNA fragments into multistranded DNA structures. Biopolymers 50: 679–689.
Gourdine JP, Greenwell P, Smith-Ravin E (2005) Application of recombinant phage display antibody system in study of Codakia orbicularis gill proteins. Appl Biochem Biotechnol 125: 41–52.
Guo JQ, You SY, Li L, Zhang YZ, Huang JN, Zhang CY (2003) Construction and high-level expression of a single-chain Fv antibody fragment specific for acidic isoferritin in Escherichia coli. J Biotechnol 102: 177–189.
Imai S, Mukai Y, Nagano K, Shibata H, Sugita T, Abe Y, Nomura T, Tsutsumi Y, Kamada H, Nakagawa S, Tsunoda S (2006) Quality enhancement of the non-immune phage scFv library to isolate effective antibodies. Biol Pharm Bull 29: 1325–1330.

Keresztessy Z, Csosz E, Harsfalvi J, Csomos K, Gray J, Lightowlers RN, Lakey JH, Balajthy Z, Fesus L (2006) Phage display selection of efficient glutamine-donor substrate peptides for transglutaminase 2. Protein Sci 15: 2466–2480.

Kneissel S, Queitsch I, Petersen G, Behrsing O, Micheel B, Dubel S (1999) Epitope structures recognised by antibodies against the major coat protein (g8p) of filamentous bacteriophage fd (Inoviridae). J Mol Biol 288: 21–28.

Kuhn A (1987) Bacteriophage M13 procoat protein inserts into the plasma membrane as a loop structure. Science 238: 1413–1415.

Lowman HB (1997) Bacteriophage display and discovery of peptide leads for drug development. Annu Rev Biophys Biomol Struct 26: 401–424.

Maruta F, Parker AL, Fisher KD, Murray PG, Kerr DJ, Seymour LW (2003) Use of a phage display library to identify oligopeptides binding to the lumenal surface of polarized endothelium by ex vivo perfusion of human umbilical veins. J Drug Target 11: 53–59.

Schier R, Bye J, Apell G., McCall A, Adams GP, Malmqvist M, Weiner LM, Marks JD (1996) Isolation of high-affinity monomeric human anti-c-erbB-2 single chain Fv using affinity-driven selection. J Mol Biol 255: 28–43.

Shibata H, Yoshioka Y, Ikemizu S, Kobayashi K., Yamamoto Y, Mukai Y, Okamoto T, Taniai M, Kawamura M, Abe Y, Nakagawa S, Hayakawa T, Nagata S, Yamagata Y, Mayumi T, Kamada H, Tsutsumi Y (2004) Functionalization of tumor necrosis factor-alpha using phage display technique and PEGylation improves its antitumor therapeutic window. Clin Cancer Res 10: 8293–8300.

Sidhu SS (2001) Engineering M13 for phage display. Biomol Eng 18: 57–63.

Smith GP (1985) Filamentous fusion phage: novel expression vectors that display cloned antigens on the virion surface. Science 228: 1315–1317.

Stich N, Van Steen G, Schalkhammer T (2003) Design and peptide-based validation of phage display antibodies for proteomic biochips. Comb Chem High Throughput Screen 6: 67–78.

Takashima A, Mummert M, Kitajima T, Matsue H (2000) New technologies to prevent and treat contact hypersensitivity responses. Ann N Y Acad Sci 919: 205–213.

Verhaert RM, Van Duin J, Quax WJ (1999) Processing and functional display of the 86 kDa heterodimeric penicillin G acylase on the surface of phage fd. Biochem J 342: 415–422.

Yamamoto Y, Tsutsumi Y, Yoshioka Y, Nishibata T, Kobayashi K., Okamoto T, Mukai Y, Shimizu T, Nakagawa S, Nagata S, Mayumi T (2003) Site-specific PEGylation of a lysine-deficient TNF-alpha with full bioactivity. Nat Biotechnol 21: 546–552.

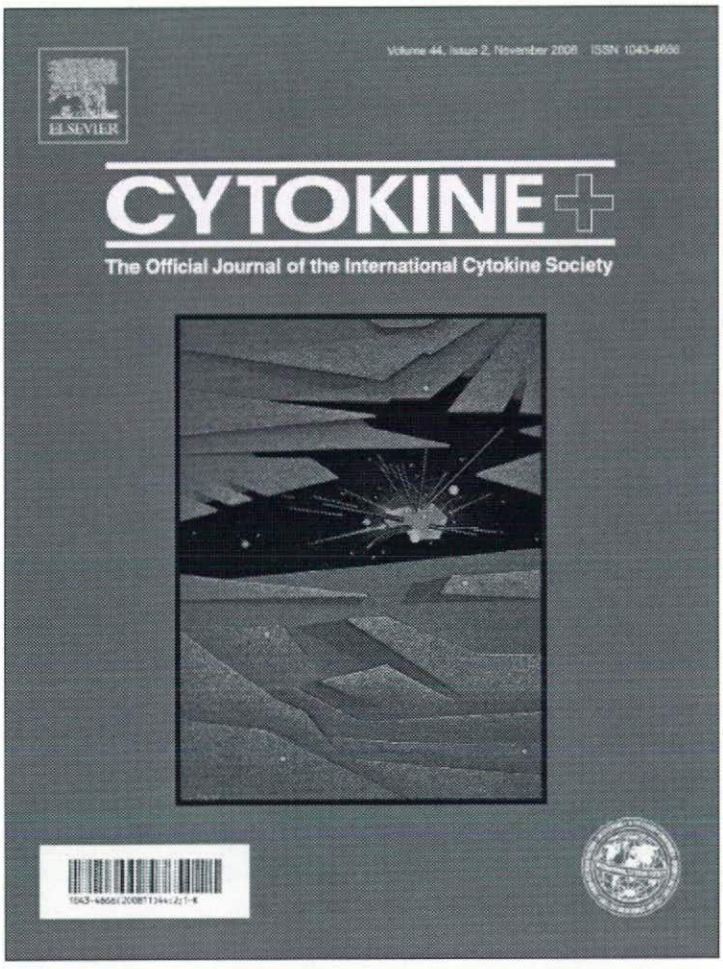

Cytokine 44 (2008) 229–233

Contents lists available at ScienceDirect

Cytokine

journal homepage: www.elsevier.com/locate/issn/10434666

The therapeutic effect of TNFR1-selective antagonistic mutant TNF-α in murine hepatitis models

Hiroko Shibata [a,b], Yasuo Yoshioka [a,c,d], Akiko Ohkawa [a,d], Yasuhiro Abe [a,d], Tetsuya Nomura [a,d], Yohei Mukai [a,d], Shinsaku Nakagawa [d], Madoka Taniai [e], Tsunetaka Ohta [e], Tadanori Mayumi [f], Haruhiko Kamada [a,c], Shin-ichi Tsunoda [a,c,*], Yasuo Tsutsumi [a,c,d]

[a] Laboratory of Pharmaceutical Proteomics, National Institute of Biomedical Innovation (NIBIO), 7-6-8 Saito-Asagi, Ibaraki, Osaka 567-0085, Japan
[b] National Institute of Health Science, Kamiyoga 1-18-1, Setagaya-ku, Tokyo 158-8501, Japan
[c] The Center for Advanced Medical Engineering and Informatics, Osaka University, 1-6 Yamadaoka, Suita, Osaka 565-0871, Japan
[d] Graduate School of Pharmaceutical Sciences, Osaka University, 1-6 Yamadaoka, Suita, Osaka 565-0871, Japan
[e] Biomedical Institute, Research Center, Hayashibara Biochemical Laboratories, Inc., 675-1 Fujisaki, Okayama 702-8006, Japan
[f] Faculty of Pharmaceutical Sciences, Kobe Gakuin University, 518 Arise, Igawadani, Nishi-ku, Kobe 651-2180, Japan

ARTICLE INFO

Article history:
Received 23 April 2008
Received in revised form 1 July 2008
Accepted 14 July 2008

Keywords:
Tumor necrosis factor-α
Liver failure
Inflammation
Therapy

ABSTRACT

Tumor necrosis factor-α (TNF-α) is critically involved in a wide variety of inflammatory pathologies, such as hepatitis, via the TNF receptor-1 (TNFR1). To develop TNFR1-targeted anti-inflammatory drugs, we have already succeeded in creating a TNFR1-selective antagonistic mutant TNF-α (R1antTNF) and shown that R1antTNF efficiently inhibits TNF-α/TNFR1-mediated biological activity in vitro. In this study, we examined the therapeutic effect of R1antTNF in acute hepatitis using two independent experimental models, induced by carbon tetrachloride (CCl_4) or concanavalin A (ConA). In a CCl_4-induced model, treatment with R1antTNF significantly inhibited elevation in the serum level of ALT (alanine aminotransferase), a marker for liver damage. In a ConA-induced T-cell-mediated hepatitis model, R1antTNF also inhibited the production of serum immune activated markers such as IL-2 and IL-6. These R1antTNF-mediated therapeutic effects were as good as or better than those obtained using conventional anti-TNF-α antibody therapy. Our results suggest that R1antTNF may be a clinically useful TNF-α antagonist in hepatitis.

1. Introduction

Acute and chronic liver failure represents a worldwide health problem in humans for which there is no effective pharmacological treatment. For example, fulminant liver failure (FLF) is a devastating liver disease that is associated with significant mortality (40–80%) worldwide [1–3]. The incidence of FLF has increased in the last decade accounting for >2000 deaths annually in the United States alone [2]. Various etiologies result in acute and chronic liver failure. Immune-mediated mechanisms play a central role in autoimmune and viral hepatitis and thus determine disease progression.

Molecules belonging to the Tumor necrosis factor (TNF) superfamily, especially TNF-α, play an integral role in the regulation of innate and adaptive immunity, as well as contributing to inflammatory responses [4,5]. Overproduction of TNF-α has been implicated in the pathogenesis of various inflammatory conditions including autoimmune diseases [4]. Recent studies suggest that TNF-α may also play a crucial role in the progression of liver failure [6–8]. Elevated levels of TNF-α occur in various acute and chronic liver diseases, including viral and alcoholic hepatitis, FLF, and exposure to hepatotoxins [9,10]. Thus, TNF-α appears to be involved in mediating hepatic cell death in experimental models of hepatitis. Furthermore, the inhibition of TNF-α by means of antibody (Ab) or soluble decoy receptors has proven to have a clinical benefit [11,12]. However, these therapies can cause serious side effects, such as bacterial and virus infection, lymphoma development, and lupus inflammatory disease, because they also inhibit the TNF-α-dependent host defense function of the patients [13,14]. TNF-α binds to two receptor-subtypes, p55 TNF receptor (TNFR1) and p75 TNF receptor (TNFR2), to exert its biological activities [15]. The two receptors have distinct biological functions with different distribution patterns; TNFR1 is constitutively expressed in most tissues, whereas expression of TNFR2 is highly regulated and is typically found in cells of the immune system [16]. It is generally believed that most of the TNF-α activities, including inflammatory responses in hepatitis, are triggered by TNFR1, whereas TNFR2 plays a pivotal role in regulating the immune response [15,17,18]. Unfortunately, the therapies with Ab or soluble decoy

* Corresponding author. Address: Laboratory of Pharmaceutical Proteomics, National Institute of Biomedical Innovation, 7-6-8 Saito-Asagi, Ibaraki, Osaka 567-0085, Japan. Fax: +81 72 641 9817.
E-mail address: tsunoda@nibio.go.jp (S. Tsunoda).

1043-4666/$ - see front matter © 2008 Elsevier Ltd. All rights reserved.
doi:10.1016/j.cyto.2008.07.003

receptors affect the TNFR2-mediated activities of TNF-α, which are essential for immune function. Therefore, these therapies also have the potential to cause serious side effects, such as an increased risk of reactivating infectious disease or lymphoma. It is hoped that these problems can be overcome by the use of TNFR1-specific agents that selectively inhibit TNF-α-bioactivity through TNFR1 without interfering with TNFR2.

We have developed a novel technology to produce TNF-α muteins which bind to independent TNFRs using a unique phage-display method [19–21]. Recently we succeeded in producing a novel TNFR1-selective antagonistic mutant TNF-α (R1antTNF) using phage-display [21]. We showed that R1antTNF displays exclusive TNFR1 selective binding, which leads to effective and selective inhibitory effects of TNFR1-mediated biological activity both in vitro and in vivo without affecting TNFR2-mediated bioactivity [21].

In this study, we examined the therapeutic effect of R1antTNF in acute hepatitis using two independent experimental models, induced by carbon tetrachloride (CCl_4) or concanavalin A (ConA). R1antTNF showed anti-inflammatory effect on both acute hepatitis models. Especially, in CCl_4-induced acute hepatitis, R1antTNF showed superior therapeutic effect compared to the common anti-TNF-α Ab. These results indicate that R1antTNF can be a clinically useful TNF-α antagonist for the treatment of inflammatory diseases such as hepatitis.

2. Materials and methods

2.1. Cytokines and antibodies

Recombinant human wild-type TNF-α (wtTNF-α) and R1antTNF were purified as previously described [21]. Briefly, recombinant TNF-α s produced in *Escherichia coli* BL21(DE3) were recovered from inclusion bodies, washed in Triton X-100 and then solubilized in 6 M guanidine–HCl, 0.1 M Tris–HCl, pH 8.0 and 2 mM EDTA. Solubilized protein at 10 mg/ml was reduced with 10 mg/ml dithioerythritol for 4 h at room temperature and refolded by 100-fold dilution in a refolding buffer; 100 mM Tris–HCl, 2 mM EDTA, 0.5 M arginine and oxidized glutathione (551 mg/l). After dialysis against 20 mM Tris–HCl pH 7.4, containing 100 mM urea, active trimeric proteins were purified by Q-Sepharose (GE Healthcare Bioscience, Tokyo, Japan) and MonoQ chromatography (GE Healthcare Bioscience). Additionally, size-exclusion chromatography (Superose 12; GE Healthcare Bioscience) was performed. The endotoxin level of the purified TNF-αs were determined to be <300 pg/mg. Anti-mouse TNF-α Ab (MP6-XT3) was purchased from BD Biosciences Pharmingen (Franklin Lakes, NJ).

2.2. Cell culture

HEp-2 cells (a human laryngeal squamous cell carcinoma cell line) were provided by Cell Resource Center for Biomedical Research (Tohoku University, Sendai, Japan) and were maintained in RPMI 1640 (Sigma–Aldrich Japan, Tokyo, Japan) supplemented with 10% FBS and antibiotics. PC60-hTNFR1(+) cells (a mouse-rat fusion hybridoma consisting of human TNFR1-expressing PC60 cells) were generously provided by Dr. Vandenabeele (University of Gent, Belgium) [22], and maintained in RPMI 1640 supplemented with 10% FBS, 1 mM sodium pyruvate, 5×10^{-5} M 2-ME, 3 mg/ml puromycin (Wako Pure Chemical Industries, Osaka, Japan) and 1% antibiotic cocktail.

2.3. Cytotoxicity assay

For the inhibition assay, human HEp-2 cells were cultured in the 96-well plates (4×10^4 cells/well) in the presence of a constant concentration of the human wtTNF-α (20 ng/ml) and a serial dilution of the R1antTNF with 100 μg/ml cycloheximide. After incubation for 18 h, cell survival was determined using the methylene blue assay as described previously [21].

2.4. PC60-hTNFR1(+) assay

PC60-hTNFR1(+) were cultured at 5×10^4 cells/well with IL-1β (2 ng/ml). To evaluate the inhibitory activity, serially diluted R1antTNF and human wtTNF-α (200 ng/ml) were added. After 24 h incubation, the amount of rat GM-CSF produced was quantified by ELISA according to the manufacturer's protocol (R&D Systems, Minneapolis, MN).

2.5. Mice

BALB/c mice (6-week-old females) were purchased from CLEA Japan (Tokyo, Japan). All experimental protocols for animal studies were in accordance with "*Principles of Laboratory Animal Care*" (National Institutes of Health publication no. 85-23, revised 1985) and our institutional guidelines.

2.6. Hepatitis model

In the CCl_4-induced hepatitis model, mice were injected intraperitoneally with CCl_4 at a dose of 0.1 ml/kg in corn oil (10 ml/kg). Control mice received only corn oil. In this model, serum TNF-α levels reached maximum levels 12 h after treatment with CCl_4. R1antTNF and anti-mouse TNF-α Ab were administered intravenously to each group at 12 h after CCl_4 administration. Blood samples were taken at 48 h after CCl_4 administration under light ether anesthesia. In the ConA-induced hepatitis model, mice were injected intravenously with ConA (0.4 mg/mouse). Anti-mouse TNF-α Ab or R1antTNF was injected intravenously at 1 h after administration of ConA. Blood samples were taken at 4 h after ConA administration under light ether anesthesia.

2.7. Measurement of serum ALT and cytokine concentrations

Serum ALT concentration was measured using a colorimetric test (Wako Pure Chemical Industries). Serum IL-2 and IL-6 were determined by sandwich ELISA kits (DuoSet ELISA Development Systems; R&D systems). Serum samples were accordingly diluted with 1% BSA in PBS and then applied to a capture antibody-coated immunoplate. All procedures were according to the manufacturer's protocol. The ELISA detection limit was 10 pg/ml.

2.8. Statistical analysis

Data are expressed as mean values ± SEM and were analyzed by the one-way ANOVA with Dunnett's post test was performed ($^*p < 0.05$ vs. control).

3. Results

3.1. Antagonistic effect of R1antTNF on wtTNF-α induced cytotoxicity and cytokine production

To confirm the potency of R1antTNF as an antagonist to the human TNFR1-specific bioactivity of wtTNF-α, we examined the inhibitory effect of R1antTNF on wtTNF-α induced cytotoxicity in HEp-2 cells. The cytotoxic activity of wtTNF-α was inhibited by R1antTNF in a dose-dependent manner. In particular, cell viability increased from 10% to 80% after treatment with R1antTNF at 3×10^5 ng/ml (Fig. 1A). R1antTNF alone showed almost no biolog-

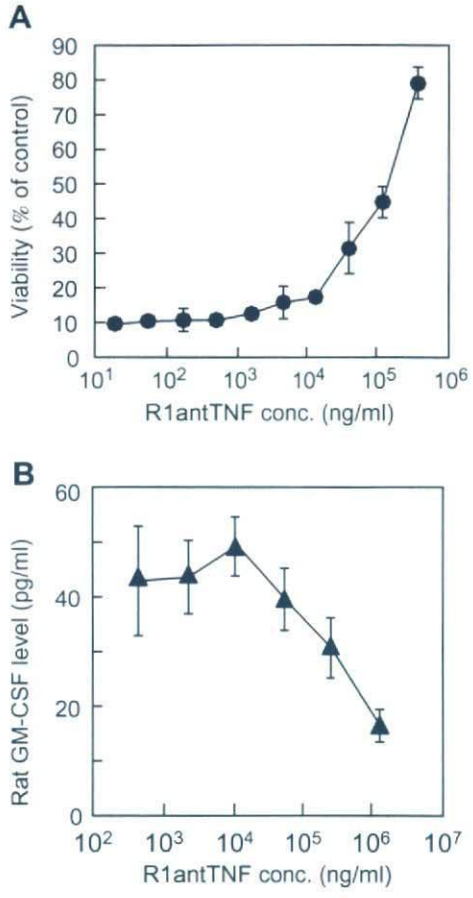

Fig. 1. Antagonistic activities of the R1antTNF. (A) Serial dilutions of R1antTNF were mixed with human wtTNF-α (20 ng/ml) and then applied to HEp-2 cells. After 18 h, the inhibitory effects of R1antTNF on the cytotoxicity of wtTNF-α were assessed by using the methylene blue assay. The absorbance of cells without wtTNF-α was plotted as 100 percent viability. (B) Serial dilutions of R1antTNF were mixed with human wtTNF-α (200 ng/ml) and applied to PC60-hTNFR1(+) cells (B). After 24 h, production of rat GM-CSF was quantified by ELISA. Rat GM-CSF was undetectable in the absence of wtTNF-α. The data represent the means ± SD ($n = 3$).

ical activity even when tested at 5×10^4 ng/ml (data not shown). We also confirmed the antagonistic effect of R1antTNF using another cell line. PC60-hTNFR1(+) cells, genetically engineered to express human TNFR1, were used to test the blocking activities of R1antTNF. R1antTNF efficiently inhibited wtTNF-α-mediated production of rat GM-CSF by PC60-hTNFR1(+) cells (Fig. 1B). The rat GM-CSF production mediated by wtTNF-α was not detected from PC60 cells, the parent cells of PC60-hTNFR1(+) cells. These results suggested that R1antTNF elicits an antagonistic effect against wtTNF-α through TNFR1.

3.2. Therapeutic effect of R1antTNF on hepatitis models

Firstly, we examined the therapeutic effect of R1antTNF in a CCl_4-induced hepatitis mouse model. CCl_4 is an industrial toxicant that is known to cause hepatic necrosis as well as free radical generation in kidney, heart, lung, testis, brain, and blood [23]. These reactive oxygen species can destroy cellular membranes, cellular proteins, and nucleic acids. The CCl_4-induced model has been extensively used as an experimental model of liver disease, such as hepatic cirrhosis and drug-induced hepatopathy. Injection of CCl_4-induced an accelerated serum ALT level, a well-characterized marker of liver damage. Treatment with R1antTNF, even at 30 μg/mouse, strongly inhibited elevation in the serum level of ALT (Fig. 2).

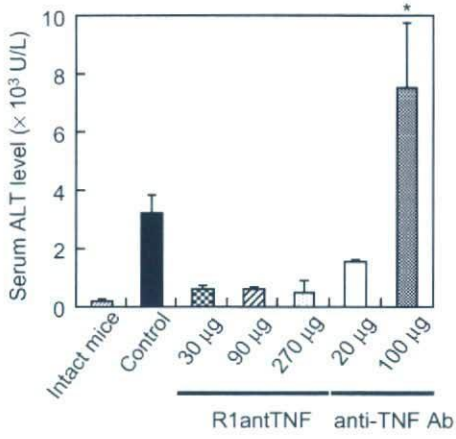

Fig. 2. Therapeutic effect of R1antTNF against the CCl_4-induced hepatitis model. BALB/c mice (6-week-old female) were intraperitoneally administered with CCl_4 at a dose of 0.1 ml/kg in corn oil (10 ml/kg). Intact animals received only corn oil. After 12 h, each mouse was given R1antTNF, anti-mouse TNF-α Ab, or PBS by intravenous injection. Blood samples were collected at 48 h after CCl_4 administration and serum ALT levels were then measured. Data represent the means ± SEM of three animals.

The serum level of ALT after treatment with R1antTNF at 30 μg/mouse was lower than that observed after treatment with anti-TNF-α Ab at 20 μg/mouse. Interestingly, treatment with the anti-TNF Ab at 100 μg/mouse actually raised the serum ALT levels compared to control mice, and seemed to even aggravate the hepatic disorder. These results indicate that R1antTNF may be more useful than anti-TNF-α Ab in treating CCl_4-induced hepatitis.

ConA-induced hepatitis in mice is a well-characterized model of T-cell-mediated liver disease and has been extensively used as a prototype mimicking human T-cell-mediated liver disease [24]. It is associated with elevated serum ALT, IL-2 and IL-6, and hepatic lesions are characterized by a massive granulocyte and T-cell infiltration, followed by hepatocyte necrosis and apoptosis. Thus, to examine the inhibitory effect of R1antTNF on Con A-induced activation of immune cells, we determined the elevation of serum IL-2 and IL-6. Initially, we examined the serum level of the T-cell-derived cytokine IL-2. R1antTNF dose-dependently reduced the level of serum IL-2 compared to control mice (Fig. 3A). The IL-2 level of mice treated with R1antTNF at 90 μg/mouse was the same as that of mice treated with anti-TNF-α Ab at 100 μg/mouse. Treatment with R1antTNF at 270 μg/mouse resulted in an even greater reduction in the serum level of IL-2. Next, to determine the inhibitory effect of R1antTNF on macrophage activation, we examined the serum IL-6 level, which is predominantly produced by Kupffer cells [25,26]. As with IL-2, R1antTNF dose-dependently reduced the serum level of IL-6 compared to control mice (Fig. 3B). The therapeutic effect thought to result from that R1antTNF inhibited ConA-induced activation of T-cells and macrophages as effectively as anti-TNF-α Ab.

4. Discussion

Previously we generated R1antTNF, a novel TNFR1-selective antagonistic mutant of TNF-α. The antagonistic effect of R1antTNF was demonstrated in vivo using a D-(+)-galactosamine (GalN)/TNF-α-dependent acute inflammatory liver injury model [21]. In this study, to clarify the therapeutic potency of R1antTNF more precisely, we examined the therapeutic effect of R1antTNF in two hepatitis models and compared the therapeutic efficacy to that of anti-TNF-α Ab.

In CCl_4-induced hepatitis model, previous study indicated that inflammatory cell influx, induction of adherent molecules in the li-

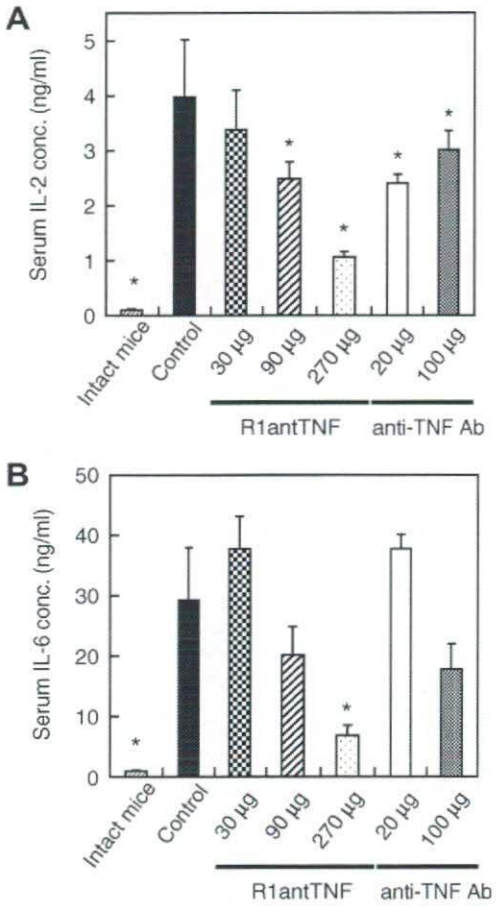

Fig. 3. Therapeutic effect of R1antTNF against ConA-induced hepatitis model. BALB/c mice (6-week-old female) were injected intravenously with ConA (0.4 mg/mouse). Anti-mouse TNF-α Ab or R1antTNF was injected 1 h after ConA injection. Blood samples were collected at 4 h after ConA injection. The serum IL-2 (A) and IL-6 (B) concentration was measured by ELISA ($n = 6$). Data represent the means ± SEM.

ver and serum ALT levels were decreased in TNFR1 knockout mice. In agreement with this, R1antTNF treatment clearly inhibited the elevation of ALT levels. However, remarkably when we used anti-TNF-α Ab as a reference for the efficacy of R1antTNF, we observed that administration of anti-TNF-α Ab increased ALT levels and even exacerbated liver failure, suggesting a paradoxical tissue protective effect of TNF-α. Similar observations were reported in a previous study, which reported that TNF-α induces the early-immediate inflammatory response through TNFR1 [27]. Additionally, it was reported that TNF-α plays an important role in the recovery from CCl_4-induced hepatitis through TNFR2 [28]. Thus, treatment with anti-TNF-α Ab may lead to adverse effects due to the lack of receptor-subtype specificity. These results indicate that R1antTNF may be more useful than anti-TNF-α Ab in treating TNFR1-dependent inflammatory diseases.

T-cell-mediated immune responses play a central role in hepatocellular injury induced by autoimmune hepatitis, viral infection, alcohol consumption, and hepatotoxins [29,30]. For example, $CD4^+$ T-cells are the predominant population of T-cells infiltrating into the liver in human autoimmune liver disease [31]. Therefore, we examined the therapeutic effect of R1antTNF on ConA-induced hepatitis model. R1antTNF inhibited the elevation of IL-2 and IL-6, which is mainly secreted from activated T-cells and Kupffer cells respectively. The therapeutic effect of R1antTNF on ConA-induced hepatitis model is almost the same as that of anti-TNF-α Ab. Numerous reports have shown that treatment with LPS or TNF-α in conjunction with D-galactosamine results in acute liver apoptosis and liver failure predominantly through TNFR1, resulting in activation of caspases and subsequent hepatocyte apoptosis [32,33]. However, studies by Kollias et al., and by Grell et al. have suggested that cell-associated TNF-α signaling through TNFR2 contributes to the development of rheumatoid arthritis and hepatocyte apoptosis [34–36]. Furthermore, investigators have argued that the liver injury from ConA treatment is not solely due to secreted TNF-α acting through TNFR1, but is also cell-associated TNF-α signaling through TNFR2 [35]. Thus, although the details of TNFR2-mediated signaling on hepatotoxicity are still unclear, it has been thought that the involvement of TNFR2 is different among hepatic models. Indeed, in our experiments, the treatment with anti-TNF-α Ab, which prevents TNF-α binding on both TNFR1 and TNFR2, exacerbated CCl_4-induced hepatitis model, but did not ConA-induced hepatitis model. Therefore, the fact that R1antTNF showed a substantial therapeutic effect in several hepatitis models is significant, and indicates the possibility that R1antTNF might be effective therapeutic agent for hepatitis caused by various factors.

One of the most common ways of enhancing the plasma half-lives of proteins is to conjugate them with polyethylene glycol (PEG) [37,38]. Because random introduction of PEG at the ε-amino groups of lysine residues usually lowers the bioactivity of proteins, application of PEGylation is generally limited to a small part of the protein. To overcome these problems of PEGylation, we recently developed a novel strategy for site-specific PEGylation via lysine-deficient mutant TNF-α, in which all of the lysine residues were replaced with other amino acids [19,20]. The lysine-deficient mutant TNF-α was site-specifically mono-PEGylated at its NH_2 terminus with PEG without loss of bioactivity. This site-specific mono-PEGylated mutant TNF-α showed increased in vivo therapeutic potency compared with the unmodified wtTNF-α and randomly mono-PEGylated wtTNF-α. R1antTNF was generated using a phage library based on this lysine-deficient mutant TNF-α and all of the lysine residues of R1antTNF were replaced with other amino acids [21]. We are currently attempting to construct mono-PEGylated R1antTNF. We anticipate that PEGylated R1antTNF will further enhance the anti-inflammatory activity for use in autoimmune disease models.

In conclusion, we have shown that R1antTNF is a useful TNF-α antagonist for treatment of hepatitis. Our results indicate that the therapeutic effect of R1antTNF can be equal or superior to that of anti-TNF-α Ab in treating TNFR1-dependent inflammatory diseases.

Acknowledgments

This study was supported in part by Grants-in-Aid for Scientific Research from the Ministry of Education, Culture, Sports, Science and Technology of Japan and Japan Society for the Promotion of Science (JSPS), in part by Health Labour Sciences Research Grant from the Ministry of Health, Labor and Welfare of Japan, in part by Health Sciences Research Grants for Research on Health Sciences focusing on Drug Innovation from the Japan Health Sciences Foundation, and in part by JSPS Research Fellowships for Young Scientists from the Japan Society for the Promotion of Science.

References

[1] Galun E, Axelrod JH. The role of cytokines in liver failure and regeneration: potential new molecular therapies. Biochim Biophys Acta 2002;1592:345–58.
[2] Vaquero J, Blei AT. Etiology and management of fulminant hepatic failure. Curr Gastroenterol Rep 2003;5:39–47.
[3] Lee WM. Acute liver failure in the United States. Semin Liver Dis 2003;23:217–26.
[4] Tracey KJ, Cerami A. Tumor necrosis factor: a pleiotropic cytokine and therapeutic target. Annu Rev Med 1994;45:491–503.

[5] Aggarwal BB. Signalling pathways of the TNF superfamily: a double-edged sword. Nat Rev Immunol 2003;3:745–56.
[6] Muto Y, Nouri-Aria KT, Meager A, Alexander GJ, Eddleston AL, Williams R. Enhanced tumour necrosis factor and interleukin-1 in fulminant hepatic failure. Lancet 1988;2:72–4.
[7] Bird GL, Sheron N, Goka AK, Alexander GJ, Williams RS. Increased plasma tumor necrosis factor in severe alcoholic hepatitis. Ann Intern Med 1990;112:917–20.
[8] Gonzalez-Amaro R, Garcia-Monzon C, Garcia-Buey L, Moreno-Otero R, Alonso JL, Yague E, et al. Induction of tumor necrosis factor alpha production by human hepatocytes in chronic viral hepatitis. J Exp Med 1994;179:841–8.
[9] Bradham CA, Plumpe J, Manns MP, Brenner DA, Trautwein C. Mechanisms of hepatic toxicity. I. TNF-induced liver injury. Am J Physiol 1998;275: G387–92.
[10] McClain CJ, Song Z, Barve SS, Hill DB, Deaciuc I. Recent advances in alcoholic liver disease. IV. Dysregulated cytokine metabolism in alcoholic liver disease. Am J Physiol Gastrointest Liver Physiol 2004;287:G497–502.
[11] Menon KV, Stadheim L, Kamath PS, Wiesner RH, Gores GJ, Peine CJ, et al. A pilot study of the safety and tolerability of etanercept in patients with alcoholic hepatitis. Am J Gastroenterol 2004;99:255–60.
[12] Carroll MB, Bond MI. Use of tumor necrosis factor-alpha inhibitors in patients with chronic hepatitis B infection. Semin Arthritis Rheum 2008, in press.
[13] Keane J, Gershon S, Wise RP, Mirabile-Levens E, Kasznica J, Schwieterman WD, et al. Tuberculosis associated with infliximab, a tumor necrosis factor alpha-neutralizing agent. N Engl J Med 2001;345:1098–104.
[14] Shakoor N, Michalska M, Harris CA, Block JA. Drug-induced systemic lupus erythematosus associated with etanercept therapy. Lancet 2002;359:579–80.
[15] Aggarwal BB, Eessalu TE, Hass PE. Characterization of receptors for human tumour necrosis factor and their regulation by gamma-interferon. Nature 1985;318:665–7.
[16] Wajant H, Pfizenmaier K, Scheurich P. Tumor necrosis factor signaling. Cell Death Differ 2003;10:45–65.
[17] MacEwan DJ. TNF receptor subtype signalling: differences and cellular consequences. Cell Signal 2002;14:477–92.
[18] Bradley J. TNF-mediated inflammatory disease. J Pathol 2008;214:149–60.
[19] Yamamoto Y, Tsutsumi Y, Yoshioka Y, Nishibata T, Kobayashi K, Okamoto T, et al. Site-specific PEGylation of a lysine-deficient TNF-alpha with full bioactivity. Nat Biotechnol 2003;21:546–52.
[20] Shibata H, Yoshioka Y, Ikemizu S, Kobayashi K, Yamamoto Y, Mukai Y, et al. Functionalization of tumor necrosis factor-alpha using phage display technique and PEGylation improves its antitumor therapeutic window. Clin Cancer Res 2004;10:8293–300.
[21] Shibata H, Yoshioka Y, Ohkawa A, Minowa K, Mukai Y, Abe Y, et al. Creation and X-ray structure analysis of the tumor necrosis factor receptor-1-selective mutant of a tumor necrosis factor-alpha antagonist. J Biol Chem 2008;283:998–1007.
[22] Vandenabeele P, Declercq W, Vanhaesebroeck B, Grooten J, Fiers W. Both TNF receptors are required for TNF-mediated induction of apoptosis in PC60 cells. J Immunol 1995;154:2904–13.
[23] Recknagel RO, Glende Jr EA, Dolak JA, Waller RL. Mechanisms of carbon tetrachloride toxicity. Pharmacol Ther 1989;43:139–54.
[24] Tiegs G, Hentschel J, Wendel A. A T cell-dependent experimental liver injury in mice inducible by concanavalin A. J Clin Invest 1992;90:196–203.
[25] Mizuhara H, O'Neill E, Seki N, Ogawa T, Kusunoki C, Otsuka K, et al. T cell activation-associated hepatic injury: mediation by tumor necrosis factors and protection by interleukin 6. J Exp Med 1994;179:1529–37.
[26] Wolf AM, Wolf D, Rumpold H, Ludwiczek S, Enrich B, Gastl G, et al. The kinase inhibitor imatinib mesylate inhibits TNF-{alpha} production in vitro and prevents TNF-dependent acute hepatic inflammation. Proc Natl Acad Sci USA 2005;102:13622–7.
[27] Bruccoleri A, Gallucci R, Germolec DR, Blackshear P, Simeonova P, Thurman RG, et al. Induction of early-immediate genes by tumor necrosis factor alpha contribute to liver repair following chemical-induced hepatotoxicity. Hepatology 1997;25:133–41.
[28] Yamada Y, Fausto N. Deficient liver regeneration after carbon tetrachloride injury in mice lacking type 1 but not type 2 tumor necrosis factor receptor. Am J Pathol 1998;152:1577–89.
[29] Kita H, Mackay IR, Van De Water J, Gershwin ME. The lymphoid liver: considerations on pathways to autoimmune injury. Gastroenterology 2001;120:1485–501.
[30] Heneghan MA, McFarlane IG. Current and novel immunosuppressive therapy for autoimmune hepatitis. Hepatology 2002;35:7–13.
[31] Lohr HF, Schlaak JF, Lohse AW, Bocher WO, Arenz M, Gerken G, et al. Autoreactive CD4+ LKM-specific and anticlonotypic T-cell responses in LKM-1 antibody-positive autoimmune hepatitis. Hepatology 1996;24:1416–21.
[32] Rothe J, Lesslauer W, Lotscher H, Lang Y, Koebel P, Kontgen F, et al. Mice lacking the tumour necrosis factor receptor 1 are resistant to TNF-mediated toxicity but highly susceptible to infection by Listeria monocytogenes. Nature 1993;364:798–802.
[33] Nowak M, Gaines GC, Rosenberg J, Minter R, Bahjat FR, Rectenwald J, et al. LPS-induced liver injury in D-galactosamine-sensitized mice requires secreted TNF-alpha and the TNF-p55 receptor. Am J Physiol Regul Integr Comp Physiol 2000;278:R1202–9.
[34] Grell M, Douni E, Wajant H, Lohden M, Clauss M, Maxeiner B, et al. The transmembrane form of tumor necrosis factor is the prime activating ligand of the 80 kDa tumor necrosis factor receptor. Cell 1995;83:793–802.
[35] Kusters S, Tiegs G, Alexopoulou L, Pasparakis M, Douni E, Kunstle G, et al. In vivo evidence for a functional role of both tumor necrosis factor (TNF) receptors and transmembrane TNF in experimental hepatitis. Eur J Immunol 1997;27:2870–5.
[36] Alexopoulou L, Pasparakis M, Kollias G. A murine transmembrane tumor necrosis factor (TNF) transgene induces arthritis by cooperative p55/p75 TNF receptor signaling. Eur J Immunol 1997;27:2588–92.
[37] Yoshioka Y, Tsutsumi Y, Nakagawa S, Mayumi T. Recent progress on tumor missile therapy and tumor vascular targeting therapy as a new approach. Curr Vasc Pharmacol 2004;2:259–70.
[38] Mukai Y, Yoshioka Y, Tsutsumi Y. Phage display and PEGylation of therapeutic proteins. Comb Chem High Throughput Screen 2005;8:145–52.

BIOCHEMICAL PHARMACOLOGY 75 (2008) 1639–1648

available at www.sciencedirect.com

ScienceDirect

journal homepage: www.elsevier.com/locate/biochempharm

Domain mapping of a claudin-4 modulator, the C-terminal region of C-terminal fragment of *Clostridium perfringens* enterotoxin, by site-directed mutagenesis

Azusa Takahashi [a], *Eriko Komiya* [a], *Hideki Kakutani* [b], *Takeshi Yoshida* [b], *Makiko Fujii* [a], *Yasuhiko Horiguchi* [c], *Hiroyuki Mizuguchi* [d,e], *Yasuo Tsutsumi* [d,f], *Shin-ichi Tsunoda* [f], *Naoya Koizumi* [a], *Katsuhiro Isoda* [b], *Kiyohito Yagi* [b], *Yoshiteru Watanabe* [a], *Masuo Kondoh* [b,*]

[a] *Department of Pharmaceutics and Biopharmaceutics, Showa Pharmaceutical University, Tokyo 194-8543, Japan*
[b] *Laboratory of Bio-Functional Molecular Chemistry, Graduate School of Pharmaceutical Sciences, Osaka University, Osaka 565-0871, Japan*
[c] *Department of Molecular Bacteriology, Division of Infectious Diseases, Osaka University, Osaka 565-0871, Japan*
[d] *Graduate School of Pharmaceutical Sciences, Osaka University, Osaka 565-0871, Japan*
[e] *Laboratory of Gene Transfer and Regulation, National Institute of Biomedical Innovation, Osaka 567-0085, Japan*
[f] *Laboratory of Pharmaceutical Proteomics, National Institute of Biomedical Innovation, Osaka 567-0085, Japan*

ARTICLE INFO

Article history:
Received 17 November 2007
Accepted 21 December 2007

Keywords:
Clostridium perfringens enterotoxin
Tight junction
Claudin
Site-directed mutagenesis

ABSTRACT

A C-terminal fragment of *Clostridium perfringens* enterotoxin (C-CPE) is a modulator of claudin-4. We previously found that upon deletion of the C-terminal 16 amino acids, C-CPE lost its ability to modulate claudin-4. Tyrosine residues in the 16 amino acids were involved in the modulation of claudin-4. In the present study, we performed functional domain mapping of the 16-amino acid region of C-CPE by replacing individual amino acids with alanine. To evaluate the ability of the alanine-substituted mutants to interact with claudin-4, we carried out a competition analysis using claudin-4-targeting protein synthesis inhibitory factor. We found that Tyr306Ala, Tyr310Ala, Tyr312Ala, and Leu315Ala mutants had reduced binding to claudin-4 compared to C-CPE. Next, we investigated effects of each alanine-substituted mutant on the TJ-barrier function in Caco-2 monolayer cells. The TJ-disrupting activity of C-CPE was reduced by the Tyr306Ala and Leu315Ala substitutions. Enhancement of rat jejunal absorption was also decreased by each of these mutations. The double mutant Tyr306Ala/Leu315Ala lost the ability to interact with claudin-4, modulate TJ-barrier function, and enhance jejunal absorption. These data indicate that Tyr306 and Leu315 are key residues in the modulation of claudin-4 by C-CPE. This information should be useful for the development of a novel claudin modulator based on C-CPE.

* *Corresponding author.* Tel.: +81 6 6879 8196; fax: +81 6 6879 8199.
E-mail address: masuo@phs.osaka-u.ac.jp (M. Kondoh).

Abbreviations: TJ, tight junction; C-CPE, C-terminal fragment of *Clostridium perfringens* enterotoxin; CPE, *Clostridium perfringens* enterotoxin; SDS-PAGE, sodium dodecyl sulfate-polyacrylamide gel electrophoresis; C-CPE-PSIF, C-CPE-fused protein synthesis inhibitory factor; LDH, lactate dehydrogenase; TEER, transepithelial electric resistance; FD-4, fluorescein isothiocyanate-dextran with a molecular weight of 4000.

0006-2952/$ – see front matter
doi:10.1016/j.bcp.2007.12.016

1. Introduction

Sequencing of the human genome has provided useful information about molecular targets for drug development and has enabled target molecule-based drug discovery. Many drug candidates, however, are eliminated during clinical development due to severe side effects caused by inadequate pharmacokinetic properties and biodistribution [1,2]. The ability of a drug to pass through epithelial and/or endothelial cell sheets is a critical aspect of its pharmacokinetics and biodistribution.

There are two routes by which drugs across epithelial and endothelial cell sheets: transcellular and paracellular. In the transcellular route, drugs are delivered by simple diffusion into the cell membranes and active transport via a receptor or transporter on cell membranes [3,4]. Transcellular delivery via transporters has been widely investigated, and the transporters involved in the influx and efflux of peptides and organic anions and cations have been identified [4–8]. The expression profiles of the transporters differ among tissues, and therefore methods for delivering drugs to a target tissue using a specific transporter may be promising; however, it may be necessary to modify the drug to target it to the appropriate transporter. Such modifications should not affect the pharmaceutical activity of the drug. Thus, the transcellular route is not always suitable for drugs created by genome-based high-throughput production.

In the paracellular route, a drug is delivered to cells by loosening the tight junctions (TJs), which normally restrict the movement of substances through the intercellular space in epithelial and endothelial cell sheets [9,10]. Therefore, to deliver drugs through the paracellular route, it is necessary to modulate the TJ-barrier function. TJ modulators have been developed as enhancers of absorption since the 1960s [11–13]. These absorption enhancers include chelators and surfactants, and they enhance absorption by dilating TJs, allowing drugs to enter the intercellular spaces of epithelial cell sheets [14]. Because opening of TJs is suitable for delivering a variety of molecules, absorption enhancers can be used for drug candidates created by genome-based high-throughput production; however their use is limited because they cause severe side effects, including exfoliation of the intestinal epithelium, irreversibly compromising its barrier functions, and because they have low tissue specificity [14–16].

As mentioned above, TJs form an intercellular seal and control solute movement through the paracellular route across epithelium and endothelium, thus maintaining the composition of the tissue interior [17,18]. There are some differences in the permeability of the TJ barrier in different types of epithelium and endothelium due to their specific physiological requirements [9]. This implies that a molecule regulating the tissue-specific barrier function of TJs should be useful for the delivery of drugs via the paracellular route.

Studies by Tsukita and co-workers have revealed that claudin plays a pivotal role in regulation of the TJ barrier [18]. Claudins are four-transmembrane proteins with molecular masses of ~23 kDa and form a large family with at least 24 members [19]. The expression of each claudin family member varies by cell type and tissue [17,20]. For instance, claudin-1 is ubiquitously expressed, whereas claudin-16 and claudin-6 are expressed in specific cell types and during specific periods of development, respectively [21,22]. Interestingly, the barrier functions of claudin are also tissue-specific. Deletion of claudin-1 and claudin-5 results in disruption of the epidermal and blood–brain barrier, respectively [23,24]. Moreover, claudins form homo/hetero-paired strands in the membrane between adjacent cells [25,26]. Because there are at least 24 claudin family members, many different strand pairs could be formed, which could give TJs a high degree of tissue specificity. The ability to modulate the barrier-function of claudin in a member-specific manner would allow tissue-specific delivery of drugs through the paracellular pathway.

Clostridium perfringens enterotoxin (CPE) causes food poisoning in humans. It consists of two functional domains, an N-terminal cytotoxic region and a C-terminal receptor-binding region (C-CPE) [27–29]. A receptor for CPE was identified in 1997 [30], and it was found to be identical to claudin-4 in 1999 [20]. Treatment of cells with C-CPE causes a decrease in intracellular claudin-4 levels and disruption of the TJ barrier in epithelial cell sheets [31]. Using C-CPE as a claudin modulator, we previously showed that it is possible to enhance drug absorption by 400-fold compared to sodium caprate, the only absorption enhancer used in the clinic [32]. Thus, claudin is a novel target molecule for drug delivery through the paracellular pathway.

Currently, C-CPE is the only known modulator of claudin. Functional domain mapping of C-CPE is useful for development of a claudin modulator using C-CPE as a prototype. Indeed, we previously found that upon deletion of the C-terminal 16 amino acids, C-CPE loses its ability to modulate claudin-4. Tyr306 is a key residue for claudin-4 modulation by C-CPE [32,33]. In the present study, we performed systemic analyses of each of the C-terminal 16 amino acids. We found that Leu315 in addition to Tyr306 is important for the ability of C-CPE to modulate the TJ barrier.

2. Materials and methods

2.1. Materials

Anti-His-tag and anti-claudin-4 antibodies were obtained from Novagen (Madison, WI) and Zymed Laboratories (South San Francisco, CA), respectively. Ni-NTA agarose and PD-10 columns were purchased from Invitrogen (Carlsbad, CA) and GE Healthcare Bio-Sciences Co. (Piscataway, NJ), respectively. The reagents used in this study were of research grade.

2.2. Cell cultures

Human intestinal Caco-2 cells at passages 68–80 were used for transepithelial electrical resistance (TEER) assays. Claudin-4-expressing mouse fibroblast cells (CL4/L cells) were kindly provided by Drs. S. Tsukita and M. Furuse (Kyoto University, Japan). Caco-2 cells were cultured in Dulbecco's modified Eagle's medium containing 10% fetal bovine serum in a 5% CO_2 atmosphere at 37 °C. CL4/L cells were maintained in modified Eagle's medium containing 10% fetal bovine serum at 37 °C.

2.3. Preparation of C-CPE mutants

Each of the C-terminal 16 amino acids of C-CPE were individually mutated to Ala by polymerase chain reaction (PCR) using the primers listed in Tables 1 and 2 for single and double mutants, respectively, and pET-H_{10}PER as a template as follows [30]. The resulting PCR fragments encoding the Ala-substituted mutants were ligated into the pET-16b vector (Novagen) via the NdeI/BamHI site, and the DNA sequence was confirmed. Each plasmid was transduced into *Escherichia coli* BL21 (DE3), and production of mutant C-CPEs was induced by addition of isopropyl-β-D-thiogalactopyranoside. The harvested cells were lysed in buffer A (10 mM Tris–HCl [pH 8.0], 400 mM NaCl, 5 mM $MgCl_2$, 10% glycerol, 0.1 mM *p*-amidinophenyl methanesulfonyl fluoride hydrochloride, and 1 mM β-mercaptoethanol), supplemented with 8 M urea when necessary. The lysates were applied to a HiTrap™ Chelating HP (GE Healthcare), and mutant C-CPEs were eluted with buffer A containing 100–1000 mM imidazole. The buffer was exchanged with phosphate-buffered saline by gel filtration using a PD-10 column. The concentrations of mutant C-CPEs were estimated using a protein assay kit with bovine serum albumin as a standard (Bio-Rad, Hercules, CA). The purification of mutant C-CPEs was confirmed by sodium dodecyl sulfate-polyacrylamide gel electrophoresis (SDS-PAGE), followed by staining of the gels with Coomassie Brilliant Blue (data not shown).

2.4. Competition assay

We previously prepared C-CPE-fused protein synthesis inhibitory factor (C-CPE-PSIF), which is a claudin-4-targeting molecule, and we showed that it is cytotoxic to CL4/L cells [34]. To assess the interaction between mutant C-CPEs and claudin-4, we evaluated the competitive inhibition of C-CPE-PSIF-induced cytotoxicity by mutant C-CPEs as follows. CL4/L cells were pretreated with C-CPE or mutant C-CPE at the indicated concentrations for 1 h, after which C-CPE-PSIF was added to the cells. After an additional 36 h of culture, the cytotoxicity of C-CPE-PSIF was assayed by the release of lactate dehydrogenase (LDH) using a CytoTox96 Non-Radioactive Cytotoxicity Assay kit according to the manufacturer's protocol (Promega, Madison, WI). The cytotoxicity was expressed according to the following equation: % maximum LDH release = 100 × (LDH released from the mutant-treated CL4/L cells/the total LDH content in the cells).

2.5. Pull-down assay

Confluent Caco-2 cells, which develop TJs, were harvested and lysed in lysis buffer (phosphate-buffered saline containing 1% Triton X-100 and 1% protease inhibitor cocktail [Sigma, St. Louis, MO]). The resultant Caco-2 lysates were used for pull-down assay. Epithelial cell layers in rat jejunum were recovered and lysed in lysis buffer (25 mM Tris–HCl [pH 8.0], 150 mM NaCl, 5 mM EDTA, 1% Triton X-100, 0.5% sodium deoxycholate, 1% protease inhibitor cocktail). The buffer of the rat lysates was changed into phosphate-buffered saline by gel filtration using a PD-10 column. The resultant lysates of rat jejunum were used for pull-down assay. C-CPE or mutant C-CPEs were incubated with the lysates for 30 min at 37 °C and then mixed with Ni-NTA agarose (Invitrogen). After an additional 3 h at 4 °C, the beads were washed, and bound proteins were analyzed by SDS-PAGE followed by Western blotting using anti-claudin-4 and anti-His-tag antibodies. The bound primary antibody

Table 1 – Primers used for alanine scan

Primers	Sequences (5′–3′)
Common forward primer	ggaattc catatg gaa aga tgt gtt tta aca gtt cca tct aca
Reverse primer for Ser304Ala	cg ggatcc tta aaa ttt ttg aaa taa tat tga ata agg gta att tcc act ata tat *gca* att agc ttt cat tac aag aac
Ser305Ala	cg ggatcc tta aaa ttt ttg aaa taa tat tga ata agg gta att tcc act ata *tgc* tga att agc ttt cat tac aag
Tyr306Ala	cg ggatcc tta aaa ttt ttg aaa taa tat tga ata agg gta att tcc act *agc* tga tga att agc ttt cat tac
Ser307Ala	cg ggatcc tta aaa ttt ttg aaa taa tat tga ata agg gta att tcc *agc* ata tga tga att agc ttt c
Gly308Ala	cg ggatcc tta aaa ttt ttg aaa taa tat tga ata agg gta att *tgc* act ata tga tga att agc ttt
Asn309Ala	cg ggatcc tta aaa ttt ttg aaa taa tat tga ata agg gta *tgc* tcc act ata tga tga att agc
Tyr310Ala	cg ggatcc tta aaa ttt ttg aaa taa tat tga ata agg *tgc* att tcc act ata tga tga
Pro311Ala	cg ggatcc tta aaa ttt ttg aaa taa tat tga ata *tgc* gta att tcc act ata tga tga
Tyr312Ala	cg ggatcc tta aaa ttt ttg aaa taa tat tga *agc* agg gta att tcc act ata tga
Ser313Ala	cg ggatcc tta aaa ttt ttg aaa taa tat *tgc* ata agg gta att tcc act ata
Ile314Ala	cg ggatcc tta aaa ttt ttg aaa taa *tgc* tga ata agg gta att tcc act
Leu315Ala	cg ggatcc tta aaa ttt ttg aaa *tgc* tat tga ata agg gta att tcc
Gln317Ala	cg ggatcc tta aaa ttt *tgc* aaa taa tat tga ata agg gta att
Lys318Ala	cg ggatcc tta aaa *tgc* ttg aaa taa tat tga ata agg gta att
Phe319Ala	cg ggatcc tta *agc* ttt ttg aaa taa tat tga ata agg gta att

The underlined sequence in the common forward primer indicates the NdeI site. The underlined sequence in the reverse primers and the italicized codon indicate the BamHI site and the alanine-substituted residue, respectively.

Table 2 – Primers and templates used for preparation of double-alanine mutants

Primers or templates	Sequence (5′–3′)/template
Common forward primer	ggaattc catatg gaa aga tgt gtt tta aca gtt cca tct aca
Tyr306Ala/Leu315Ala	
Reverse primer	cg ggatcc tta aaa ttt ttg aaa *tgc* tat tga ata agg gta att tcc
Template	Tyr306Ala
Tyr310Ala/Leu315Ala	
Reverse primer	cg ggatcc tta aaa ttt ttg aaa *tgc* tat tga ata agg *ggc* att tcc
Template	Tyr310Ala
Tyr312Ala/Leu315Ala	
Reverse primer	cg ggatcc tta aaa ttt ttg aaa *tgc* tat tga *agc* agg gta att tcc
Template	Tyr312Ala

The underlined sequence in the forward and reverse primer indicate NdeI and BamHI sites, respectively. The italicized sequences in the reverse primers indicate the sites of mutation. The templates was pET-16b vector containing the indicated mutant C-CPE.

was detected with a peroxidase-labeled secondary antibody followed by visualization with chemiluminescence reagents (Amersham Bioscience, Piscataway, NJ).

2.6. TEER assay

Caco-2 cells were seeded in Transwell™ chambers (Corning, NY) at a subconfluent density. TEER of the Caco-2 monolayer cell sheets on the chamber, a sign of TJ integrity, was measured using a Millicell-ERS epithelial volt-ohmmeter (Millipore, Bedford, MA). When the TEER values reached a plateau and the TJs were well developed, the Caco-2 monolayers were treated with C-CPE or mutant C-CPEs on the apical side of the chamber, and the TEER values were measured. The TEER values were normalized by the area of the Caco-2 monolayer. The TEER value of a blank Transwell™ chamber (background) was subtracted.

2.7. In situ loop assay

The experimental protocol for the in situ loop assay was approved by the Ethics Committee of Showa Pharmaceutical University. Wistar male rats (250–280 g; Animal and Material Laboratories, Inc., Tokyo, Japan) were allowed at least a week to adapt in an environmentally controlled room. Fluorescein isothiocyanate-dextran with a molecular weight of 4000 (FD-4) was used as a model drug that passes across the intestinal epithelium mainly through the paracellular route [35–37]. Rats were anesthetized with thiamylal sodium (Mitsubishi Pharma Co. Ltd., Osaka, Japan). A midline abdominal incision was made, and the lumen of the jejunum was washed with phosphate-buffered saline. A jejunal loop (5 cm in length) was prepared by closing both ends with sutures. A mixture of FD-4 and C-CPEs was administered into the jejunal loop. Blood was collected from the jugular vein at the indicated time points. The plasma concentration of FD-4 was determined with a fluorescence spectrophotometer (Fluoroskan Ascent FL; Thermo Electron Corp., Waltham, MA). The area under the plasma concentration-time curve from 0 to 4 h (AUC_{0-4}) was calculated by the trapezoidal method.

2.8. Statistical analysis

Significant difference is evaluated by ANOVA followed by student *t*-test, and the significant difference is set at $p < 0.05$.

3. Results

3.1. Alanine scan of the C-terminal 16 amino acids in C-CPE

We previously found that upon deletion of the 16 C-terminal amino acids, C-CPE loses its ability to disrupt the TJ barrier and to interact with claudin-4, and tyrosine residues in the 16 amino acids are involved in its modulation of claudin-4 [38]. However, systematic analysis of the 16 amino acids has never been performed. To examine the function of each of the 16 amino acids, we generated mutants in which the individual amino acids were replaced with alanine. Of the 16 mutants, all except for Phe316Ala, could be expressed in *E. coli* BL21 (DE3). Thus, we were not able to examine the role of Phe316.

We previously prepared the claudin-4-targeting cytotoxic recombinant protein C-CPE-PSIF [34]. To screen the interaction of the mutants with claudin-4, we examined their ability to reduce C-CPE-PSIF-induced cytotoxicity in claudin-4-expressing CL4/L cells. Treatment of the cells with C-CPE-PSIF induced the release of approximately 55–65% of the total LDH (data not shown). The inhibition of C-CPE-PSIF-induced LDH release by each mutant C-CPE is summarized in Table 3. These results suggest that substitution of Tyr306, Tyr310, Tyr312, or Leu315 with alanine resulted in a decrease in the binding of the mutant C-CPEs to claudin-4, whereas replacement of Ser304, Ser305, Ser307, Asn309, Ser313, or Lys318 by alanine slightly increased the binding to claudin-4.

Next, we examined the effects of each mutant on the TEER value, an indicator of the tightness of the TJs. The experiments were performed using monolayers of human intestinal Caco-2 cells grown on a membrane, a method commonly used for evaluating the TJ-barrier function. Treatment of the cells with C-CPE at 20 μg/ml for 18 h lowered the TEER value from 498 to 22 Ω cm^2 (data not shown). TJ-modulating activities were calculated as the ratio of the reduction in TEER for the mutant compared to C-CPE and are presented in Table 4. Only the Tyr306Ala and Leu315Ala mutants had weaker TJ-modulating activity than C-CPE (64.1 and 45.1% of C-CPE, respectively).

3.2. Effect of Leu315Ala substitution on the ability of C-CPE to interact with claudin-4

Because of these findings, we performed further studies of the Tyr306 and Leu315 mutants. We confirmed the interaction of Tyr306Ala and Leu315Ala with claudin-4 by a pull-down assay using lysate from Caco-2 cells. Claudin-4 was precipitated by C-CPE at 1 μg/ml, whereas claudin-4 was not precipitated by Tyr306Ala or Leu315Ala at the same concentration (Fig. 1A). An

Table 3 – Competitive inhibition of C-CPE-PSIF-induced LDH release by mutant C-CPEs

Wild-type or mutant C-CPE	Inhibitory ratio (% of C-CPE)
C-CPE	100
Ser304Ala	125.6 ± 0.7
Ser305Ala	126.8 ± 0.2
Tyr306Ala	63.8 ± 0.4
Ser307Ala	123.6 ± 2.2
Gly308Ala	99.1 ± 2.7
Asn309Ala	125.6 ± 1.8
Tyr310Ala	72.2 ± 2.3
Phe311Ala	114.9 ± 0.5
Tyr312Ala	73.1 ± 2.4
Ser313Ala	132.9 ± 0.8
Ile314Ala	94.3 ± 3.1
Leu315Ala	69.1 ± 2.7
Gln317Ala	96.8 ± 1.6
Lys318Ala	126.2 ± 2.1
Phe319Ala	111.5 ± 3.9

After a 1 h of treatment with C-CPE or mutant C-CPEs at 5 μg/ml, claudin-4-exressing L cells were treated with C-CPE-PSIF (0.2 μg/ml) for 36 h, and the release of LDH was determined. The results are shown as the percent of C-CPE-induced LDH release, and the values are the means ± S.D. ($n = 4$).

Table 4 – Effects of mutant C-CPEs on TJ barrier in Caco-2 cells

Wild-type or mutant C-CPE	Decreased ratio of TEER (% of C-CPE)
C-CPE	100
Ser304Ala	100.3 ± 0.5
Ser305Ala	100.1 ± 2.3
Tyr306Ala	64.1 ± 4.3*
Ser307Ala	100.4 ± 1.8
Gly308Ala	98.1 ± 0.2
Asn309Ala	104.4 ± 1.3
Tyr310Ala	93.8 ± 1.2
Pro311Ala	101.4 ± 2.3
Tyr312Ala	100.1 ± 1.5
Ser313Ala	104.6 ± 0.8
Ile314Ala	98.3 ± 1.4
Leu315Ala	45.1 ± 5.3*
Gln317Ala	98.8 ± 1.3
Lys318Ala	99.3 ± 0.8
Phe319Ala	103.5 ± 0.9

Caco-2 cells were seeded on a Transwell™. After development of the TJ barrier in Caco-2 cells, C-CPE or mutant C-CPEs was added at 20 μg/ml, and TEER was measured. The decrease in the ratio of TEER vs. C-CPE was calculated from the following equation: 100 × (difference in TEER between 0 and 18 h after treatment of the cells with each mutant C-CPE)/(difference in TEER between 0 and 18 h after treatment with C-CPE). The values are means ± S.D. ($n = 4$).

* Significant difference from C-CPE ($p < 0.05$).

additional band was observed below claudin-4 in the pull-down assay using C-CPE and mutants. This was due to nonspecific binding of the anti-claudin-4 antibody by His-tagged protein (data not shown).

To confirm the interaction between mutated C-CPEs and claudin-4, we also investigated the dose-dependence of Tyr306Ala and Leu315Ala in a competitive assay using C-CPE-PSIF. As shown in Fig. 1B, pretreatment of the cells with C-CPE at 10 μg/ml reduced LDH release by C-CPE-PSIF from 56.5 to 8.3% of the total LDH, whereas the Tyr306Ala and Leu315Ala mutants had much weaker inhibitory effect (50.0 and 40.5% release, respectively). Thus, the interaction of C-CPE with claudin-4 was weakened by substitution of Tyr306 or Leu315 with alanine. These results suggest that Leu315 in addition to Tyr306 is important in the interaction of C-CPE with claudin-4.

We previously found that rat jejunal absorption of FD-4, a model compound used for evaluation of paracellular absorption, is enhanced by C-CPE via an interaction with claudin-4

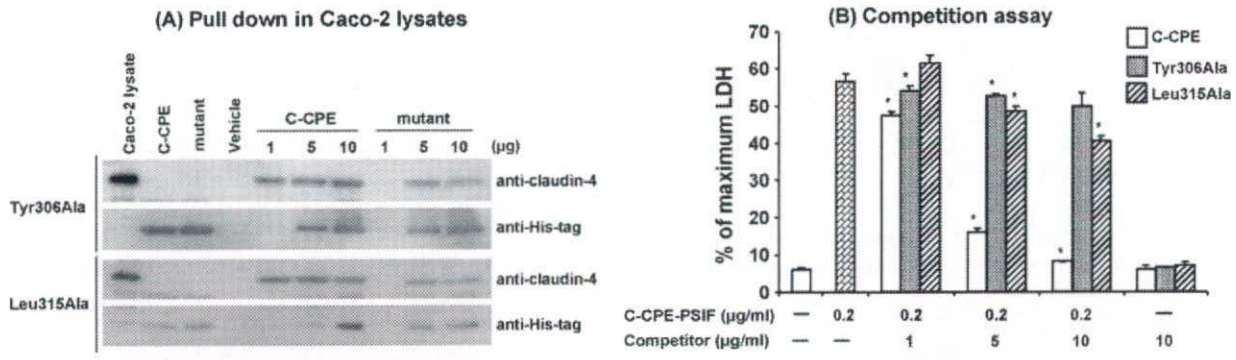

Fig. 1 – Role of Leu315 in the interaction between C-CPE and claudin-4. (A) Pull-down assay using Caco-2 lysates. TJ-developing Caco-2 cells were harvested and lysed in the lysis buffer. The lysate was incubated with vehicle, C-CPE, or mutated C-CPEs for 30 min at 37 °C. Ni-NTA agarose was added, and the mixture was incubated for 3 h at 4 °C. The Ni-NTA agarose was then precipitated, and the bound proteins were analyzed by SDS-PAGE followed by Western blotting using anti-claudin-4 or anti-His-tag antibodies. The lanes containing Caco-2 lysate, C-CPE, and mutated C-CPE (mutant) served as positive controls for claudin-4, C-CPE, and mutant C-CPEs, respectively. The results are representative of three independent experiments. (B) Competitive inhibition of C-CPE-PSIF-induced cytotoxicity by mutant C-CPEs. Claudin-4-expressing CL4/L mouse fibroblasts were pretreated with C-CPE or mutant C-CPEs at the indicated concentrations for 1 h. The cells were then incubated with C-CPE-PSIF (0.2 μg/ml). After 36 h, LDH release was determined using a commercially available kit. The results are representative of three independent experiments. Values are means ± S.D. ($n = 3$). *Significant difference from C-CPE-PSIF-treated group ($p < 0.05$).

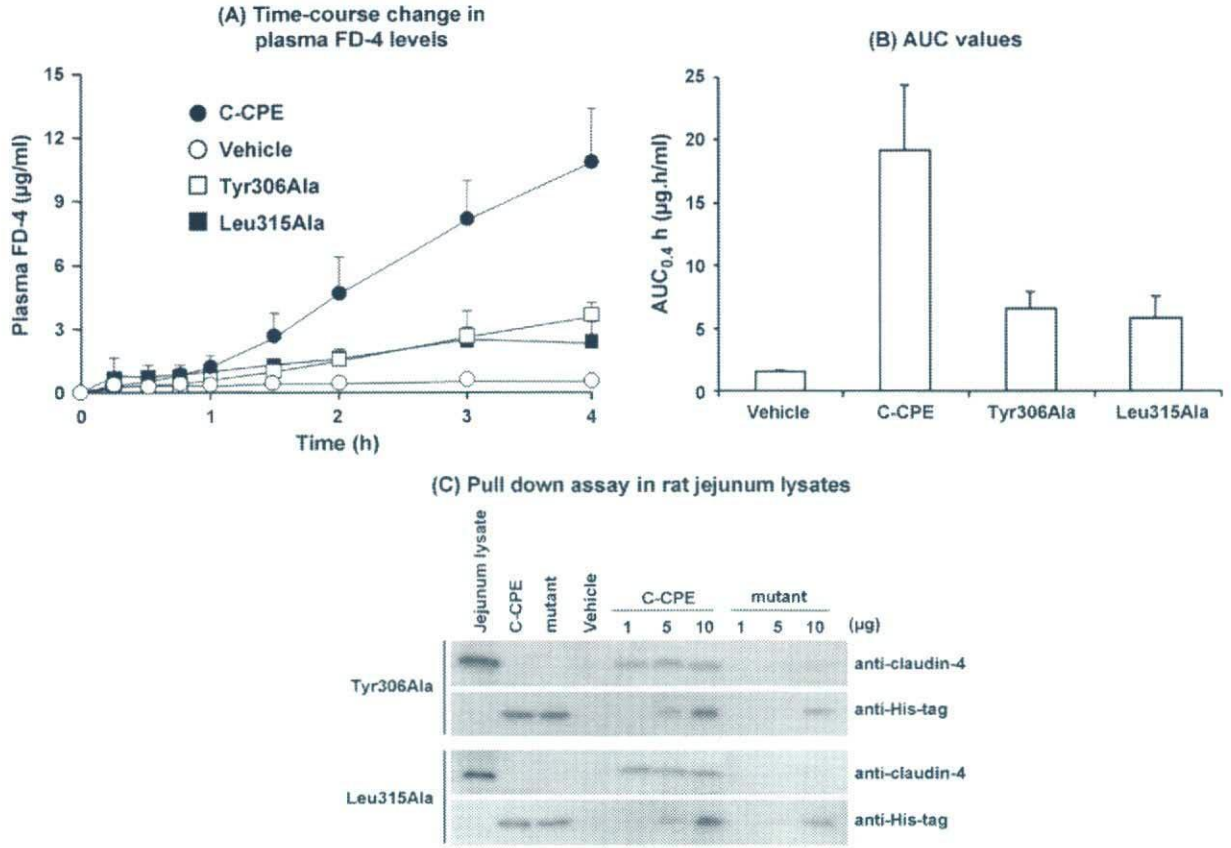

Fig. 2 – Role of Leu315 in the enhancement of absorption by C-CPE in rat jejunum. (A and B) Enhancement of jejunal absorption of FD-4 by C-CPE. The enhancement of absorption by mutant C-CPEs was evaluated by an *in situ* loop assay using rat jejunum. Briefly, rat jejunum was treated with FD-4 (10 mg/ml) in the presence of vehicle, C-CPE (0.2 mg/ml), or mutated C-CPE (0.2 mg/ml). The plasma FD-4 levels were determined at the indicated time (A), and the $AUC_{0-4\ h}$ values were calculated (B). Values are means ± S.E.M. ($n = 4$). (C) Pull-down assay in rat jejunum lysate. Mucosal epithelium in rat jejunum was recovered with a scraper and lysed in lysis buffer as described in Section 2. The lysates were incubated with C-CPE or mutated C-CPE for 30 min at 37 °C. Next, Ni-NTA agarose was added, and after a 3-h incubation at 4 °C, the precipitated Ni-NTA agarose was separated by SDS-PAGE and analyzed by Western blotting. The results are representative of three independent experiments.

[32]. We therefore examined the effect of Tyr306Ala and Leu315Ala on rat jejunal absorption of FD-4. As shown in Fig. 2A and B, C-CPE enhanced the absorption of FD-4 (12.2-fold compared to vehicle-treated controls), and Tyr306Ala and Leu315Ala had reduced abilities to enhance jejunal absorption (4.2- and 3.7-fold compared to vehicle-treated controls, respectively). To further evaluate the interaction of mutated C-CPEs with rat claudin-4, we performed a pull-down assay using rat jejunal lysate. Much less claudin-4 was precipitated by the Tyr306Ala and Leu315Ala mutants than by C-CPE, indicating that these two mutants have lower affinities for rat claudin-4 than C-CPE (Fig. 2C).

3.3. *The combination of Tyr306 and Leu315 is important for C-CPE modulation of claudin-4*

We found that ability of C-CPE to modulate claudin-4 is partially reduced by substitution of Tyr306 or Leu315 with alanine (Fig. 1 and Tables 3 and 4). We therefore evaluated whether the Leu315Ala mutation has synergistic effects by preparing double mutants Tyr306Ala/Leu315Ala, Tyr310Ala/Leu315Ala, and Tyr312Ala/Leu315Ala. Claudin-4 was precipitated by addition of Leu315Ala at 5 μg/ml but not by any of the double-alanine mutants at 10 μg/ml (Fig. 3A). Also, the double-substituted mutants did not affect C-CPE-PSIF-induced cytotoxicity even at 10 μg/ml (Fig. 3B), indicating that they lost their affinity for claudin-4.

Next, we investigated the absorption-enhancing effects of the double mutated C-CPEs using an *in situ* loop assay. Replacement of Tyr306 or Leu315 by alanine partially reduced the enhancement of absorption (Fig. 2A and B), whereas C-CPE with a combination of Leu315Ala and either Tyr306Ala, Tyr310Ala, or Tyr312Ala lost its absorption-enhancing effect (Fig. 4A and B). Similar results were obtained in the TEER assay using Caco-2 monolayers. Reduction of TEER was not observed for these double-substituted mutants (Fig. 4C). These data indicate that in addition to Tyr306, Leu315 is a key residue determining the potency of C-CPE as a modulator of the TJ barrier.

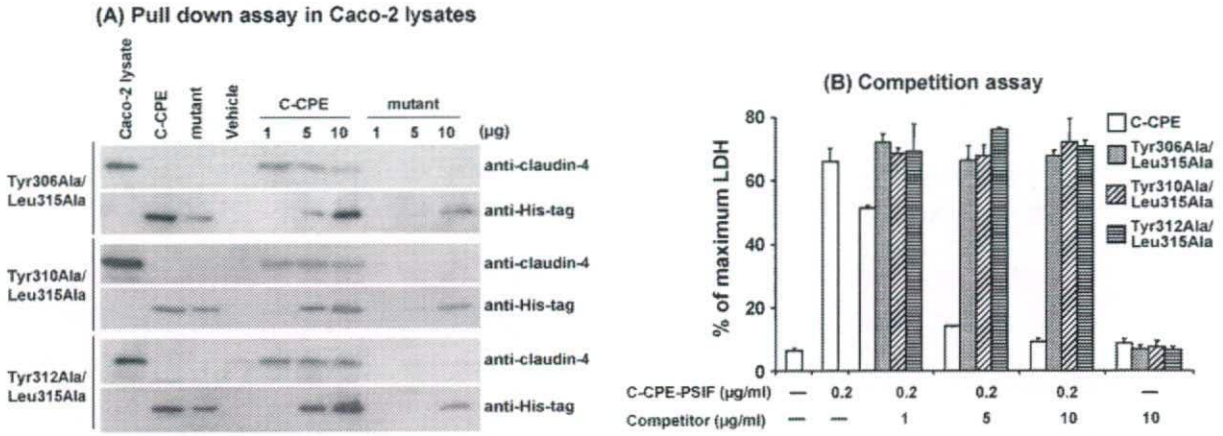

Fig. 3 – Interaction between double-substituted mutant C-CPE and claudin-4. Interaction of double-substituted mutant C-CPEs (Tyr306Ala/Leu315Ala, Tyr310Ala/Leu315Ala, and Tyr312Ala/Leu315Ala) with claudin-4 was evaluated by a pull-down assay using Caco-2 cell lysates (A) and by competitive inhibition of C-CPE-PSIF-induced cytotoxicity in CL4/L cells (B) as described in Fig. 1A and B, respectively. The results are representative of three independent experiments. In panel B, values are means ± S.D. ($n = 3$).

4. Discussion

Claudin is a promising target for developing a drug delivery system via the paracellular route. Our previous findings indicated that C-CPE is a potent modulator of claudin-4 and that the C-terminal 16 amino acids are pivotal for modulation of claudin-4 by C-CPE [32,38]. We have also evaluated the role of tyrosine residues within these 16 C-terminal amino acids by alanine scanning [33,39]. In the present study, we carried out a systematic functional domain mapping of these 16 amino acid residues. We found that Leu315 in addition to Tyr306 is pivotal for the interaction between C-CPE and claudin-4 and for modulation of the TJ barrier by C-CPE.

Functional domain mapping is needed for the development of claudin modulators based on C-CPE. We therefore screened for residues involved in binding of C-CPE to claudin-4 by a competition assay. We found that some mutants, such as Ser307Ala and Lys318Ala, had a slightly higher affinity for claudin-4 than C-CPE (Table 3). We did not focus on these mutants in the current studies, but it will be interesting to examine this further in future studies. We also found that substitution of Ser307 or Lys318 with alanine did not affect the abilities of C-CPE to modulate the TJ barrier and interact with claudin-4 in a pull-down assay (Table 4 and data not shown, respectively). Thus, at least, Ser307 and Lys318 do not appear to be essential for the activities of C-CPE. The results of our systematic domain mapping studies of the C-terminal 16 amino acids in C-CPE from the current study and from our previous report are summarized in Table 5 [33,38]. They suggest that multiple residues in C-CPE, especially Tyr306 and Leu315, are critical for the modulation of claudin-4.

Like Tyr306Ala, the Leu315Ala mutant had the reduced abilities to bind claudin-4, modulate the TJ barrier, and enhance absorption compared to those of C-CPE. The precise mechanism by which C-CPE disrupts the TJ barrier is still unclear. Sonoda et al. found that treatment of MDCK cells with C-CPE caused the disappearance of claudin-4 from TJs and a decrease in intracellular claudin-4 protein levels, indicating that claudin-4 may be degraded after its interaction with C-CPE [31]. Claudin-4 contains a signal sequence for sorting to clathrin-coated vesicles (a ALGVLL motif at amino acids 92–97 and a YVGW motif at amino acids 165–168) [40,41]. It is possible that C-CPE-bound claudin-4 is taken up by clathrin-mediated endocytosis. Indeed, Matsuda et al. showed that endocytosis of claudins occurs during the remodeling of TJs [42].

Do Tyr306 and Leu315 have the same function? Substitution of Tyr306 or Leu315 in C-CPE with alanine resulted in a partial reduction in the ability of C-CPE to modulate claudin-4, and the effects of double alanine-substitution were

Table 5 – Summary of functional domain mapping in the C-terminal 16 amino acids of C-CPE

Amino acid residue	Binding to claudin	Modulation of TJ barrier	Jejunal absorption	Source
Tyr306	Yes	Yes	Yes	This study, Harada et al. [33]
Tyr310	Yes	No	No	Harada et al. [33]
Tyr312	Yes	No	Yes	Harada et al. [33]
Leu315	Yes	Yes	Yes	This study

Binding to claudin was assessed using a competition assay using C-CPE-PSIF, modulation of TJ barrier was determined using a TEER assay using Caco-2 monolayer, and jejunal absorption based on an *in situ* loop assay using rat jejunum. Yes and No indicate important and not important for each function of C-CPE, respectively.

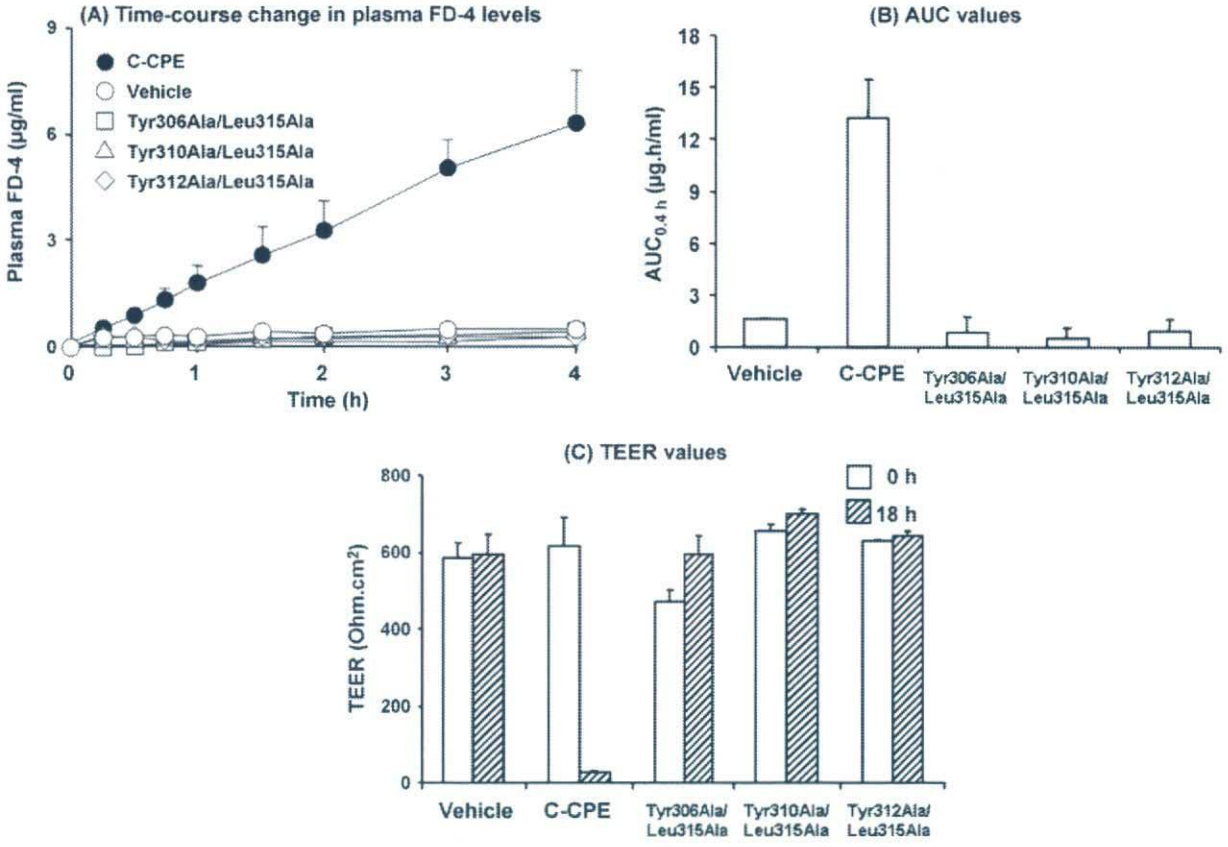

Fig. 4 – Modulation of TJ barrier by double-substituted mutant C-CPEs. (A and B) Enhancement of absorption by double-mutated C-CPEs in rat jejunum. Time-course of plasma FD-4 levels (A) and $AUC_{0-4\ h}$ values (B) were evaluated as described in Fig. 2A and B. Values are means ± S.E.M. ($n = 4$). (C) TEER assay in Caco-2 monolayer cells. Caco-2 cells were grown on Transwell™ filters. After TJs were developed, vehicle, C-CPE or mutated C-CPEs was added at 20 μg/ml, and TEER values were measured after 0 and 18 h. Values are means ± S.D. ($n = 4$).

additive (Fig. 4), suggesting that these two residues interact with claudin-4 at different sites or in different ways. Substitution of Tyr306 with Phe (aromatic and hydrophobic residue) and Trp (aromatic, hydrophobic, and polar residue) but not Lys (polar and cationic residue) did not affect the binding of C-CPE to claudin-4 or the modulation of the TJ barrier [39]. Taken together, these findings suggest that C-CPE interact with claudin-4 on the membrane through a hydrophobic cluster formed by the side-chains of Tyr at position 306 and Leu at position 315. Double substitution of Leu315 and Tyr310 or Tyr312 with alanine caused a loss of activities, indicating that the two residues equally and cooperatively contribute to modulation of claudin-4 by C-CPE. Indeed, triple- or quadruple-alanine mutants at Tyr306, Tyr310, Tyr312, and Leu315 lack activities like the double mutants (data not shown).

Other than the functional analyses of C-CPE, little is known about mode of action of C-CPE as a claudin modulator. Determination of the three-dimensional structure of claudin and C-CPE/CPE should help elucidate the mechanism by which C-CPE modulates claudin-4, but the tertiary structures of claudin and CPE have not yet been solved. Very recently, Van Itallie et al. reported structure of the C-terminal claudin-binding domain of CPE [43]. The structure has a nine strand β sandwich, and the claudin-4-binding site is on a loop domain between β8 and β9 strands. Tyr306, Tyr310 and Tyr312 exist on the loop domain, and Leu315 exists in the β9 strand. Our data is consistent with the putative claudin-4-binding domain by the structural analysis.

In conclusion, we carried out the complete fine mapping of the C-terminal 16 amino acids of C-CPE to determine their roles in claudin-4 modulation. We found that Leu315 plays a pivotal role in the modulation of claudin-4 by C-CPE. Together, our previous and current results indicate that Tyr at positions 306, 310, and 312 and Leu at position 315 of C-CPE participate in the modulation of claudin-4. These findings should help in the development of a novel claudin modulator based on C-CPE.

Acknowledgements

We thank Y. Hattori, A. Koyama, and A. Itoh for their kind support. We thank Drs. S. Tsukita and M. Furuse for providing us with CL4/L cells. This study was partly supported by a Grant-in-Aid from the Ministry of Education, Science, and Culture of Japan, Mochida Memorial Foundation for Medical and Pharmaceutical Sciences, Takeda Science Foundation,

Cosmetology Research Foundation, Shiseido Grant for Scientific Research, Tokyo Biochemical Research Foundation, Senri Life Science Foundation, and Astellas Foundation for Research on Metabolic Disorders.

REFERENCES

[1] White RE. High-throughput screening in drug metabolism and pharmacokinetic support of drug discovery. Annu Rev Pharmacol Toxicol 2000;40:133–57.
[2] Roberts SA. High-throughput screening approaches for investigating drug metabolism and pharmacokinetics. Xenobiotica 2001;31:557–89.
[3] Majumdar S, Duvvuri S, Mitra AK. Membrane transporter/receptor-targeted prodrug design: strategies for human and veterinary drug development. Adv Drug Deliv Rev 2004;56:1437–52.
[4] Mizuno N, Niwa T, Yotsumoto Y, Sugiyama Y. Impact of drug transporter studies on drug discovery and development. Pharmacol Rev 2003;55:425–61.
[5] Inui KI, Masuda S, Saito H. Cellular and molecular aspects of drug transport in the kidney. Kidney Int 2000;58:944–58.
[6] Koepsell H. Organic cation transporters in intestine, kidney, liver, and brain. Annu Rev Physiol 1998;60:243–66.
[7] Meijer DK, Hooiveld GJ, Schinkel AH, van Montfoort JE, Haas M, de Zeeuw D, et al. Transport mechanisms for cationic drugs and proteins in kidney, liver and intestine: implication for drug interactions and cell-specific drug delivery. Nephrol Dial Transplant 1999;14(Suppl. 4):1–3.
[8] Van Aubel RA, Masereeuw R, Russel FG. Molecular pharmacology of renal organic anion transporters. Am J Physiol 2000;279:F216–32.
[9] Powell DW. Barrier function of epithelia. Am J Physiol 1981;241:G275–88.
[10] Anderson JM, Van Itallie CM. Tight junctions and the molecular basis for regulation of paracellular permeability. Am J Physiol 1995;269:G467–75.
[11] Tidball CS, Lipman RI. Enhancement of jejunal absorption of heparinoid by sodium ethylenediaminetetraacetate in the dog. Proc Soc Exp Biol Med 1962;111:713–5.
[12] Engel RH, Riggi SJ. Effect of sulfated and sulfonated surfactants on the intestinal absorption of heparin. Proc Soc Exp Biol Med 1969;130:879–84.
[13] Aungst BJ. Intestinal permeation enhancers. J Pharm Sci 2000;89:429–42.
[14] Hochman J, Artursson P. Mechanisms of absorption enhancement and tight junction regulation. J Control Release 1994;29:253–67.
[15] Yamamoto A, Uchiyama T, Nishikawa R, Fujita T, Muranishi S. Effectiveness and toxicity screening of various absorption enhancers in the rat small intestine: effects of absorption enhancers on the intestinal absorption of phenol red and the release of protein and phospholipids from the intestinal membrane. J Pharm Pharmacol 1996;48:1285–9.
[16] Kondoh M, Takahashi A, Fujii M, Yagi K, Watanabe Y. A novel strategy for a drug delivery system using a claudin modulator. Biol Pharm Bull 2006;29:1783–9.
[17] Van Itallie CM, Anderson JM. Claudins and epithelial paracellular transport. Annu Rev Physiol 2006;68:403–29.
[18] Furuse M, Tsukita S. Claudins in occluding junctions of humans and flies. Trends Cell Biol 2006;16:181–8.
[19] Furuse M, Fujita K, Hiiragi T, Fujimoto K, Tsukita S. Claudin-1 and -2: novel integral membrane proteins localizing at tight junctions with no sequence similarity to occludin. J Cell Biol 1998;141:1539–50.
[20] Morita K, Furuse M, Fujimoto K, Tsukita S. Claudin multigene family encoding four-transmembrane domain protein components of tight junction strands. Proc Natl Acad Sci USA 1999;96:511–6.
[21] Simon DB, Lu Y, Choate KA, Velazquez H, Al-Sabban E, Praga M, et al. Paracellin-1, a renal tight junction protein required for paracellular Mg^{2+} resorption. Science 1999;285:103–6.
[22] Turksen K, Troy TC. Claudin-6: a novel tight junction molecule is developmentally regulated in mouse embryonic epithelium. Dev Dyn 2001;222:292–300.
[23] Furuse M, Hata M, Furuse K, Yoshida Y, Haratake A, Sugitani Y, et al. Claudin-based tight junctions are crucial for the mammalian epidermal barrier: a lesson from claudin-1-deficient mice. J Cell Biol 2002;156:1099–111.
[24] Nitta T, Hata M, Gotoh S, Seo Y, Sasaki H, Hashimoto N, et al. Size-selective loosening of the blood–brain barrier in claudin-5-deficient mice. J Cell Biol 2003;161:653–60.
[25] Furuse M, Sasaki H, Tsukita S. Manner of interaction of heterogeneous claudin species within and between tight junction strands. J Cell Biol 1999;147:891–903.
[26] Furuse M, Furuse K, Sasaki H, Tsukita S. Conversion of zonulae occludentes from tight to leaky strand type by introducing claudin-2 into Madin-Darby canine kidney I cells. J Cell Biol 2001;153:263–72.
[27] Horiguchi Y, Uemura T, Kamata Y, Kozaki S, Sakaguchi G. Production and characterization of monoclonal antibodies to *Clostridium perfringens* enterotoxin. Infect Immun 1986;52:31–5.
[28] Hanna PC, Mietzner TA, Schoolnik GK, McClane BA. Localization of the receptor-binding region of *Clostridium perfringens* enterotoxin utilizing cloned toxin fragments and synthetic peptides. The 30 C-terminal amino acids define a functional binding region. J Biol Chem 1991;266:11037–43.
[29] Hanna PC, Wieckowski EU, Mietzner TA, McClane BA. Mapping of functional regions of *Clostridium perfringens* type A enterotoxin. Infect Immun 1992;60:2110–4.
[30] Katahira J, Inoue N, Horiguchi Y, Matsuda M, Sugimoto N. Molecular cloning and functional characterization of the receptor for *Clostridium perfringens* enterotoxin. J Cell Biol 1997;136:1239–47.
[31] Sonoda N, Furuse M, Sasaki H, Yonemura S, Katahira J, Horiguchi Y, et al. *Clostridium perfringens* enterotoxin fragment removes specific claudins from tight junction strands: evidence for direct involvement of claudins in tight junction barrier. J Cell Biol 1999;147:195–204.
[32] Kondoh M, Masuyama A, Takahashi A, Asano N, Mizuguchi H, Koizumi N, et al. A novel strategy for the enhancement of drug absorption using a claudin modulator. Mol Pharmacol 2005;67:749–56.
[33] Harada M, Kondoh M, Ebihara C, Takahashi A, Komiya E, Fujii M, et al. Role of tyrosine residues in modulation of claudin-4 by the C-terminal fragment of *Clostridium perfringens* enterotoxin. Biochem Pharmacol 2007;73:206–14.
[34] Ebihara C, Kondoh M, Hasuike N, Harada M, Mizuguchi H, Horiguchi Y, et al. Preparation of a claudin-targeting molecule using a C-terminal fragment of *Clostridium perfringens* enterotoxin. J Pharmacol Exp Ther 2006;316:255–60.
[35] Sallee VL, Wilson FA, Dietschy JM. Determination of unidirectional uptake rates for lipids across the intestinal brush border. J Lipid Res 1972;13:184–92.

[36] Utoguchi N, Watanabe Y, Shida T, Matsumoto M. Nitric oxide donors enhance rectal absorption of macromolecules in rabbits. Pharm Res 1998;15:870–6.
[37] Ohtake K, Natsume H, Ueda H, Morimoto Y. Analysis of transient and reversible effects of poly-L-arginine on the in vivo nasal absorption of FITC-dextran in rats. J Control Release 2002;82:263–75.
[38] Takahashi A, Kondoh M, Masuyama A, Fujii M, Mizuguchi H, Horiguchi Y, et al. Role of C-terminal regions of the C-terminal fragment of *Clostridium perfringens* enterotoxin in its interaction with claudin-4. J Control Release 2005;108:56–62.
[39] Ebihara C, Kondoh M, Harada M, Fujii M, Mizuguchi H, Tsunoda S, et al. Role of Tyr306 in the C-terminal fragment of *Clostridium perfringens* enterotoxin for modulation of tight junction. Biochem Pharmacol 2007;73:824–30.
[40] Bonifacino JS, Traub LM. Signals for sorting of transmembrane proteins to endosomes and lysosomes. Annu Rev Biochem 2003;72:395–447.
[41] Ivanov AI, Nusrat A, Parkos CA. Endocytosis of epithelial apical junctional proteins by a clathrin-mediated pathway into a unique storage compartment. Mol Biol Cell 2004;15:176–88.
[42] Matsuda M, Kubo A, Furuse M, Tsukita S. A peculiar internalization of claudins, tight junction-specific adhesion molecules, during the intercellular movement of epithelial cells. J Cell Sci 2004;117:1247–57.
[43] Van Itallie CM, Betts L, Smedley 3rd JG, McClane BA, Anderson JM. Structure of the claudin-binding domain of *Clostridium perfringens* enterotoxin. J Biol Chem 2008;283:268–74.

Available online at www.sciencedirect.com
ScienceDirect
European Journal of Pharmaceutics and Biopharmaceutics 70 (2008) 1–6
European Journal of Pharmaceutics and Biopharmaceutics
www.elsevier.com/locate/ejpb

Research paper

Evaluation of promoter strength in mouse and rat primary hepatocytes using adenovirus vectors

Eri Arita [a,1], Masuo Kondoh [a,1], Katsuhiro Isoda [a], Hikaru Nishimori [a], Takeshi Yoshida [a], Hiroyuki Mizuguchi [b,c], Kiyohito Yagi [a,*]

[a] *Laboratory of Bio-Functional Molecular Chemistry, Graduate School of Pharmaceutical Sciences, Osaka University, Osaka, Japan*
[b] *National Institute of Biomedical Innovation, Osaka, Japan*
[c] *Graduate School of Pharmaceutical Sciences, Osaka University, Osaka, Japan*

Received 5 October 2007; accepted in revised form 17 March 2008
Available online 29 March 2008

Abstract

Primary cultured hepatocytes are widely used in the studies of basic and clinical hepatology. Finding an efficient method for gene transfer into primary hepatocytes will be an important advance for these studies. In the present study, we evaluated the activity of an adenovirus vector including promoters for the Rous sarcoma virus (RSV), elongation factor 1α, and cytomegalovirus (CMV) as well as the β-actin promoter/CMV enhancer (CA) using β-galactosidase as a reporter gene. Although RSV and elongation factor 1α promoters had low transcriptional activity in hepatocytes, the CA and CMV promoters had high activity. The CA promoter was the most active, mediating 50.3- and 204.4-fold more activity than the RSV promoter in mouse and rat hepatocytes, respectively. Dose-response studies revealed that transgene activity can be controlled by as much as 1000-fold, by selection of the promoter and the number of infectious particles per cell. These findings should help in the construction of adenovirus vectors for expressing genes of interest in rodent primary cultured hepatocytes.

Keywords: Hepatocyte; Adenovirus vector; Promoter; Transgene activity

1. Introduction

The liver is a multifunctional and vital organ that consists of parenchymal and nonparenchymal cells such as sinusoidal endothelial, Kupffer, and stellate cells. Hepatocytes have been well studied, and they are known to play a central role in the metabolism of drugs and detoxification of xenobiotics. Because there are few hepatocyte cell lines that have similar characteristics and behavior as intact hepatocytes, primary cultures of hepatocytes have been used for the study of viral hepatitis and the regeneration, physiology, pathobiology, and pharmacology of the liver [1–5]; however, primary hepatocytes progressively lose the liver-specific properties when isolated and cultivated [1,6]. The ectopic expression of genes of interest is very useful for estimation and investigation of the roles and functions of the genes, and an extremely efficient transfection system is needed for research using primary hepatocytes.

Gene transduction techniques include both nonviral and viral vectors. Adenovirus (Ad) vectors are widely used for basic and clinical research and are 100- to 1000-fold more efficient at mediating gene transduction than cationic lip-

Abbreviations: RSV, rous sarcoma virus; CMV, cytomegalovirus; CA, β-actin promoter/CMV enhancer; Ad, adenovirus; RT-PCR, reverse transcription polymerase chain reaction; CAR, coxsackievirus and adenovirus receptor; GAPDH, glyceraldehyde-3-phosphate dehydrogenase; EF, elongation factor 1α; Ad, adenovirus; LacZ, β-galactosidase; X-gal, 5-bromo-4-chloro-3-indolyl-β-D-galactopyranoside.

* Corresponding author. Laboratory of Bio-Functional Molecular Chemistry, Graduate School of Pharmaceutical Sciences, Osaka University, Suita, Osaka 565-0871, Japan. Tel.: +81 6 6879 8195; fax: +81 6 6879 8199.
E-mail address: yagi@phs.osaka-u.ac.jp (K. Yagi).

[1] These authors equally contribute to this study.

0939-6411/$ - see front matter © 2008 Elsevier B.V. All rights reserved.
doi:10.1016/j.ejpb.2008.03.013